

Effects of interaural decoherence on sensitivity to interaural level differences across frequency

Andrew D. Brown^{1,a)} and Daniel J. Tollin²

¹Department of Speech and Hearing Sciences, University of Washington, 1417 Northeast 42nd Street, Seattle, Washington 98105, USA

²Department of Physiology and Biophysics, University of Colorado School of Medicine, Aurora, Colorado 80045, USA

ABSTRACT:

The interaural level difference (ILD) is a robust indicator of sound source azimuth, and human ILD sensitivity persists under conditions that degrade normally-dominant interaural time difference (ITD) cues. Nonetheless, ILD sensitivity varies somewhat with both stimulus frequency and interaural correlation (coherence). To further investigate the combined binaural perceptual influence of these variables, the present study assessed ILD sensitivity at frequencies 250–4000 Hz using stimuli of varied interaural correlation. In the first of two experiments, ILD discrimination thresholds were modestly elevated, and subjective lateralization slightly reduced, for both half-correlated and uncorrelated narrowband noise tokens relative to correlated tokens. Different from thresholds in the correlated condition, which were worst at 1000 Hz [Grantham, D.W. (1984). *J. Acoust. Soc. Am.* **75**, 1191–1194], thresholds in the decorrelated conditions were independent of frequency. However, intrinsic envelope fluctuations in narrowband stimuli caused moment-to-moment variation of the nominal ILD, complicating interpretation of measured thresholds. Thus, a second experiment employed low-fluctuation noise tokens, revealing a clear effect of interaural decoherence *per se* that was strongly frequency-dependent, decreasing in magnitude from low to high frequencies. Measurements are consistent with known integration times in ILD-sensitive neurons and also suggest persistent influences of covert ITD cues in putative “ILD” tasks. © 2021 Acoustical Society of America.

<https://doi.org/10.1121/10.0005123>

(Received 22 July 2020; revised 27 April 2021; accepted 10 May 2021; published online 30 June 2021)

[Editor: Jonas Braasch]

Pages: 4630–4648

I. INTRODUCTION

When a sound source is located to the side of an observer, the signal arriving at the ear farther from the source is delayed and attenuated relative to that nearer the source. The resultant interaural timing and level differences (ITDs and ILDs) provide the major acoustic cues to sound source location in the horizontal plane (Rayleigh, 1907). The availability and utility of each cue depends on a variety of factors, including the source signal’s spectrotemporal profile, acoustic environment (which affects the impinging signal’s spectrotemporal profile), and the hearing status of the observer. In general, low-frequency ITD cues dominate perception when they are available (Wightman and Kistler, 1992; Macpherson and Middlebrooks, 2002), particularly at signal onsets or during rising envelope segments (Dietz *et al.*, 2013; Stecker and Bibee, 2014; reviewed in Stecker *et al.*, 2021). However, ITD sensitivity can be profoundly affected by temporal distortions of the signal (e.g., echoes and reverberation or interaural decorrelation; Jeffress *et al.*, 1962; Devore *et al.*, 2009; Rakerd and Hartmann, 2010; see Brown *et al.*, 2015), by aging and other factors that affect hearing status (e.g., Grose and Mamo, 2010, Papesh *et al.*,

2017; Bernstein and Trahiotis, 2019), and by the effective stimulus frequency (either waveform or envelope) at which the ITD cue is conveyed (Zwislocki and Feldman, 1956; Hafter and Dye, 1983; Brughera *et al.*, 2013).

Compared to ITD sensitivity, ILD sensitivity is much less variable across frequency (Mills, 1960; Jones *et al.*, 2015), age and other impacts on hearing status (e.g., Babkoff *et al.*, 2002; Litovsky *et al.*, 2010; but see Bernstein and Trahiotis, 2019), and various temporal manipulations that dramatically impact ITD detection (cf. Rakerd and Hartmann, 1985; Hartmann and Constan, 2002; Stecker and Brown, 2012). Nonetheless, ILD sensitivity is reduced under some conditions. For example, the acuity of ILD perception decreases with an increasing ILD magnitude (Hafter *et al.*, 1977; Yost and Dye, 1988; see Brown *et al.*, 2018), and the resultant variation in sensitivity across azimuth may exceed that observed for ITD (Carlile *et al.*, 2016). Although inherently dependent on the integration of the fluctuating signals at the two ears (Tollin, 2003; Owruksy *et al.*, 2021), ILD sensitivity also appears to depend on the moment-to-moment temporal similarity of the signals at the two ears, i.e., the interaural correlation. In one study, threshold ILDs for broadband or low-pass noise tokens were elevated by a small (<0.5 dB) amount when uncorrelated tokens were presented to the two ears (Hartmann and Constan, 2002). A slightly larger effect (~1 dB) was elicited in a later study

^{a)}Also at: Virginia Merrill Bloedel Hearing Research Center, University of Washington, Seattle, WA 98195, USA.

Electronic mail: andrewdb@uw.edu, ORCID: 0000-0003-0838-2894.

using high-frequency narrowband tokens with explicitly decorrelated envelopes (Brown and Tollin, 2016). While pointing to the broader conclusion that the ILD system is capable of extracting usable information from temporally degraded signals that lack stable long-term ITD cues, the foregoing data also suggest that inputs sufficiently interaurally “mismatched” in time can modestly degrade sensitivity to ILD.

A rather more mysterious—and remarkably reproducible—influence on ILD sensitivity is stimulus frequency. Numerous studies over a period of several decades have demonstrated an increase in ILD thresholds in the vicinity of 1000 Hz (e.g., Mills, 1960; Grantham, 1984; Yost and Dye, 1988; Goupell and Rosen, 2016). Whereas the magnitude of this “1000-Hz bump” in thresholds (or, equivalently, 1000 Hz “slump” in acuity) is typically modest in absolute terms (~ 1 dB), it can represent a two- or threefold change relative to thresholds at nearby frequencies. This result, though considered explicitly in one study (Grantham, 1984), remains unexplained. Accounts of physiological ILD sensitivity do not predict non-monotonicity at low frequencies (Jones *et al.*, 2015; Tollin, 2003), and it is particularly notable that ILD thresholds *improve* at very low frequencies (≤ 500 Hz), even as both hearing (audibility) thresholds and ITD thresholds deteriorate (Zwislocki and Feldman, 1956). Although ILD is conventionally viewed as a high-frequency cue and low-frequency ILD sensitivity has been studied comparatively little, large low-frequency ILDs are, in fact, common for sources near (≤ 1 m from) the head (Brungart and Rabinowitz, 1999) and in multisource environments (Młynarski and Jost, 2014), and some evidence suggests that even small low-frequency ILD cues can significantly influence sound source localization (e.g., Hartmann *et al.*, 2016). Ecological implications aside, the frequency-dependence of ILD sensitivity in the vicinity of 1000 Hz remains a perplexing psychoacoustic result and an unexplained detail of binaural hearing.

The present study examined the joint effects of stimulus frequency and interaural correlation on listeners’ sensitivity to ILD. In two separate experiments, ILD discrimination and lateralization were measured at frequencies from 250 to 4000 Hz using stimuli with varied interaural correlation and envelope characteristics. Data provide insight on temporal constraints on ILD sensitivity across frequency and also suggest persistent binaural perceptual influences of covert low-frequency ITD cues—that is, ITD cues that are not explicitly manipulated but that may nonetheless affect performance—which should be considered when making putative “ILD” measurements.

II. METHODS

A. Subjects

Thirteen adult human subjects (seven female) participated in one of two experiments. All subjects reported normal hearing and demonstrated pure-tone audiometric thresholds < 20 dB hearing level (HL) with ≤ 10 dB

interaural asymmetry at octave frequencies over the range 250–8000 Hz. Data were collected at two study sites; procedures for Experiment 1 were approved by the Colorado Multiple Institutional Review Board, and procedures for Experiment 2 were approved by the University of Washington Human Subjects Division. Seven subjects (including a laboratory research assistant) completed testing in Experiment 1. Six different subjects (including a different laboratory research assistant) completed testing in Experiment 2. All subjects were naive to the purpose of the experiments.

B. Stimuli

Stimuli were generated using MATLAB (MathWorks, Natick, NJ), synthesized at a sampling rate of 44.1 kHz at 16-bit resolution (Lynx TWO-A, Lynx Studio Technology, Costa Mesa, CA, or RME Fireface UC, RME GmbH, Haimhausen, Germany), and presented via circumaural headphones (Bose AE2, Bose Corp., Framingham, MA or Sennheiser HD280, Wedemark, Germany). In both Experiments 1 and 2, stimuli were narrowband noises of varied center frequency (250, 500, 1000, 1500, 2000, 3000, 4000 Hz); new noise samples (i.e., tokens) were generated online for each trial. All stimuli were 250 ms in duration with 10-ms \cos^2 on- and off-ramps and presented at a nominal level of 65 dB sound pressure level (SPL). Other token parameters differed between the two experiments as follows.

In Experiment 1, tokens were generated by digitally filtering Gaussian noise with a fourth-order bandpass Butterworth centered at the target frequency (filter coefficients obtained using the MATLAB `butter` function, “bandpass” option; filtering implemented using the `filtfilt` function). The effective stimulus bandwidth was fixed at 25 Hz. This narrow bandwidth relegated stimuli to a single auditory filter: 25 Hz is roughly one-half of the equivalent rectangular bandwidth (ERB) at the lowest tested frequency (250 Hz) and a significantly lesser fraction at the higher tested frequencies (Glasberg and Moore, 1990). In addition to restricting stimuli to a single auditory filter, use of a fixed bandwidth was intended to ensure that envelope fluctuations would remain constant (on average) across center frequency (Rice, 1954). However, the magnitude of these fluctuations was relatively large: Across a sample pool of 500 waveforms per frequency, the mean crest factor of Experiment 1 tokens was 2.70 (± 0.32 standard deviation). The mean envelope fourth moment, an alternative measure of amplitude fluctuation (see Hartmann and Pumplin, 1988; Bernstein and Trahiotis, 2007), was 1.92 (± 0.38 standard deviation). For independent (uncorrelated tokens), such amplitude fluctuation could introduce substantial fluctuation in the effective ILD over time, complicating the interpretation of measured performance (see Sec. III B).

Thus, in Experiment 2, envelope fluctuation was constrained explicitly using low-fluctuation noise (Kohlrausch *et al.*, 1997; see also Pumplin, 1985). Briefly, Gaussian

noise was digitally filtered using a sixth-order bandpass Butterworth filter to produce a 1-ERB (Glasberg and Moore, 1990) noise centered at the target frequency. This filtered token was then divided by its own Hilbert envelope, acting to flatten peaks and troughs present in the original envelope. The normalized result was then passed through the 1-ERB filter again. This process was repeated eight times, yielding a final 1-ERB token with a nearly flat amplitude envelope. From 250 to 4000 Hz, across a sample pool of 500 waveforms per frequency, the mean crest factor of the resultant signal was $1.58 (\pm 0.03 \text{ dB standard deviation})$ compared to a crest factor of 1.414 for a sinusoid. Unprocessed tokens had a mean crest factor of $3.90 (\pm 0.46 \text{ standard deviation})$. The envelope fourth moment values for the same sample were (processed low-fluctuation waveforms) $1.14 (\pm 0.005$

standard deviation) and (unprocessed waveforms) $2.03 (\pm 0.21 \text{ standard deviation})$. All Experiment 2 stimuli were saved for *post hoc* trial-by-trial analyses of binaural properties. Long-term amplitude spectra and exemplar time domain signals (upper insets) used in Experiments 1 and 2 are shown in the left and right panels of Fig. 1(A), respectively.

In the present paper, because the interaural decorrelation procedure explicitly limited the peak of the cross-correlation function, the terms “correlation” and “coherence” are used interchangeably. Correlated signals (coherence = 1.0) were generated by presenting identical tokens to each ear. Uncorrelated tokens (nominal coherence = 0.0) were generated by presenting independent tokens to each ear. Half-correlated tokens (nominal coherence = 0.5), which were

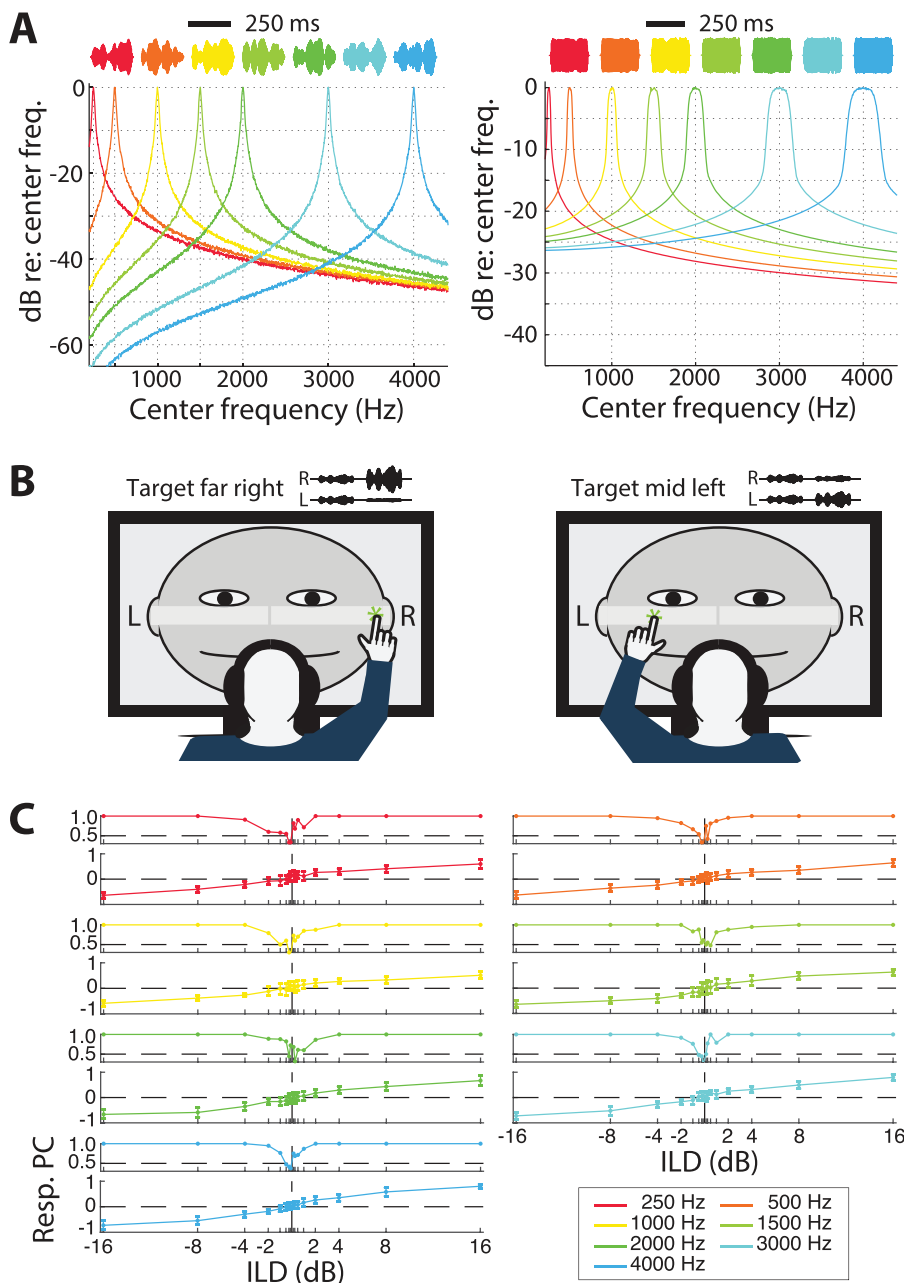


FIG. 1. Stimuli and joint discrimination-lateralization task. (A) Stimuli of the present study as illustrated in the frequency and time (upper insets) domains. (Left) Experiment 1 stimuli; the absolute bandwidth and, thus, the envelope fluctuation rate were constant across center frequency. (Right) Experiment 2 stimuli; the relative bandwidth was fixed at 1 ERB; fluctuation was explicitly constrained using a “low-fluctuation” token generation procedure (see text). (B) Subjects used a touch-sensitive display to indicate both the sidedness (discrimination) and lateral position (lateralization) of target stimuli relative to a diotic reference. (C) Obtained data, thus, consisted of both the percent-correct discrimination data (PC; upper plot in each sub-panel) and lateralization magnitude data (Resp., lower plot in each sub-panel), analyzed as described in the text.

used in Experiment 1 only, were generated by presenting a given token to one ear and a scaled copy of that token plus a second, independent token to the opposite ear (Licklider and Dzendolet, 1948; Hartmann and Cho, 2011). The online token generation script ensured that the token correlation was within ≤ 0.1 of the nominal correlation, i.e., uncorrelated stimuli had precise correlations between -0.1 and 0.1 and half-correlated stimuli had precise correlations between 0.4 and 0.6 .

C. Procedure

During each experiment, subjects were seated in a quiet (ambient sound level 15–20 dBA) room and instructed to face a touch-sensitive display (Elo 3200L, Elo Touch Solutions Inc., Milpitas, CA, or Dell P2418HT, Dell, Inc., Round Rock, TX). The monitor displayed two adjacent response panels at eye level overlaid on a cartoon illustration of a head [see Fig. 1(B)]. Each trial within a block consisted of two stimulus presentation intervals separated by a 500-ms silent period. The first interval contained the reference stimulus, which carried 0 dB ILD, and the second interval contained the target stimulus, which carried a nonzero ILD. For all center frequencies and levels of coherence, the same pair of noise tokens was used for both reference and target intervals within a trial. The target ILD was selected randomly from a set of eight ILD magnitudes: 0.125, 0.25, 0.5, 1, 2, 4, 8, and 16 dB ILD. Subjects were instructed to complete two tasks on each trial, both achieved by touching either the left or right response panel to indicate (1) whether the second (target) stimulus was to the right or left of the first (reference) stimulus—a discrimination task—and (2) how far right or left the second stimulus appeared to be located—a perceptual scaling task [see Fig. 1(B)]. The response location within each panel was measured as the normalized distance from the central edge of the bar (magnitudes spanning 0.0–1.0 with a resolution of 0.0001). Visual feedback on the discrimination response was given immediately following each response by the appearance of an asterisk at the recorded response location (green if the left/right discrimination response was correct, red if it was incorrect). ILDs randomly favored the left or right ear and were imposed symmetrically by amplifying the signal to the favored ear by half of the total ILD and attenuating the signal to the opposite ear by half of the total ILD.

Importantly, as all trials consisted of two token presentation intervals (see below), the average binaural level of each interval was randomly decremented or incremented by up to 8 dB (relative to the nominal level of 65 dB SPL) to limit the use of monaural level cues rather than the intended binaural ILD cue. The effectiveness of roving procedures in limiting useful monaural cues can be predicted *a priori* (e.g., Grantham, 1984) but because all Experiment 2 tokens were saved for later analyses, we were able to verify the effectiveness of the implemented rove values empirically: across all trials, a perfect monaural level detector (discrimination response dictated by the monaural level change

across intervals) yielded a threshold ILD of 11.0 dB, severalfold higher than the worst real (binaural) thresholds observed.

Each ILD magnitude was presented 20 times within a testing block (160 trials). Following a practice block, two blocks were completed in random order for each combination of frequency and interaural correlation. Blocks were completed over the course of several testing sessions, each ~ 2 h in length. An example dataset from a single subject in Experiment 1 is shown in Fig. 1(C).

D. Data analysis

Data were analyzed offline. Discrimination and lateralization responses were analyzed separately. To derive ILD discrimination thresholds, responses for left-favoring and right-favoring trials were combined, giving 40 total trials per ILD magnitude. Each subject's percent-correct performance was then fitted using a Weibull function (Wichmann and Hill, 2001) with a lower bound of 50% (random guessing) and upper bound of 100% (attained by all subjects at the largest tested ILDs). The threshold ILD was taken as the fitted ILD yielding 76% correct ($d' = 1$). Lateralization was assessed according to (1) the average lateralization response value (maximum possible leftward response was -1 , maximum rightward $+1$) at each ILD, (2) the standard deviation of the lateralization responses at each ILD, and (3) the slope (gradient) of the lateralization responses across ILD. Lateralization metrics were computed using responses for trials with ILD magnitudes ≥ 2 dB. While the largest ILDs were correctly discriminated regardless of interaural correlation, cues carried by correlated versus uncorrelated tokens might still give rise to different intracranial images. The average lateralization response was assumed to index the image center. The standard deviation of the lateralization response could be interpreted to index either trial-to-trial variability in a punctate intracranial image or the effective “width” of a more diffuse intracranial image with a poorly defined center. Per our own subjective experience, decorrelated stimuli indeed yielded more diffuse images, making it difficult to precisely indicate the image center. Recognizing that subjects did not indicate the image width explicitly, we thus use lateralization standard deviation as a proxy for image width and call this measure lateralization *blur*. Finally, the difference in mean responses for the largest leftward (-16 dB) and rightward ($+16$ dB) ILDs was computed to evaluate the maximum extent of lateralization produced by each stimulus type, termed lateralization *range*.

Inferential statistical testing of discrimination thresholds and lateralization metrics (across levels of interaural correlation and across frequency) were conducted using SPSS (Version 26, IBM, Inc., Armonk, NY). Tests included repeated-measures analysis of variance (ANOVA; with Greenhouse-Geisser adjusted degrees of freedom) and paired-samples *t*-tests (exact *t*-statistics and *p*-values are reported except for groups of tests for which all $p > 0.05$). Additional explanations of conducted analyses, including

post hoc stimulus-dependent analyses specific to Experiment 2, are provided in Secs. III and IV.

III. EXPERIMENT 1: NARROWBAND NOISE OF VARIED INTERUARAL CORRELATION

A. Results

ILD discrimination thresholds for Experiment 1 are shown in Fig. 2(A) [individual subjects, open symbols ($n = 7$); mean ± 1 standard error, filled symbols]. Each panel gives performance for a single frequency band with three levels of nominal interaural correlation per frequency. Performance in the correlated condition was comparable to that reported in many previous studies using tones, with thresholds in the vicinity of 1 dB ILD for most listeners and an apparent maximum of ~ 2 dB around 1000 Hz. Interaural decorrelation led to a slight elevation of thresholds (to 2–2.5 dB ILD) for most subjects at most frequencies. The effect was generally largest for the uncorrelated condition (i.e., independent tokens) but was also evident and of a similar magnitude in the half-correlated condition (nominal correlation of 0.5).

Average discrimination thresholds (± 1 standard error) are plotted as a function of the frequency in Fig. 2(B) for the correlated (filled) and uncorrelated (open) conditions, illustrating the effect of decorrelation at each frequency. Data (including thresholds for half-correlated stimuli) were submitted to a repeated-measures ANOVA with factors of frequency and interaural correlation. The main effect of interaural correlation was significant ($F_{2,8.6} = 20.39$, $p = 0.001$), whereas the main

effect of frequency and the frequency-by-interaural correlation interaction were not ($p > 0.05$). As suggested in Fig. 2(A), much of the effect of interaural decorrelation was realized with a nominal correlation of 0.5; at 500 Hz, for example, thresholds for half-correlated stimuli were, on average, 1.5 dB worse than thresholds for correlated stimuli ($t_6 = 3.02$, $p = 0.023$), but total decorrelation produced only an additional 0.1 dB decrement ($t_6 = -0.29$, $p = 0.782$).

The effects of stimulus frequency appeared to vary between correlated and uncorrelated conditions. In the correlated condition, thresholds were worse at 1000 Hz than at neighboring frequencies: paired comparisons demonstrated better thresholds in the correlated condition both one octave below (500 Hz versus 1000 Hz, $t_6 = -2.79$, $p = 0.032$) and one octave above (2000 Hz versus 1000 Hz, $t_6 = -3.43$, $p = 0.014$), reproducing the 1000-Hz bump in ILD thresholds evident in several prior studies (see the Introduction and Sec. V). These differences were not present in the uncorrelated conditions; the mean threshold at 1000 Hz was slightly better than those at neighboring frequencies in an absolute sense, and the distribution of thresholds across subjects overlapped substantially across frequency (all $p \gg 0.05$). Reasons for this frequency-invariant pattern are considered in Sec. III B.

Lateralization data for Experiment 1 are plotted in Fig. 3. Data for half-correlated stimuli were largely redundant with data for uncorrelated stimuli [as for discrimination, Fig. 2(A)] and are omitted here to enable easier visualization of differences between the correlated and

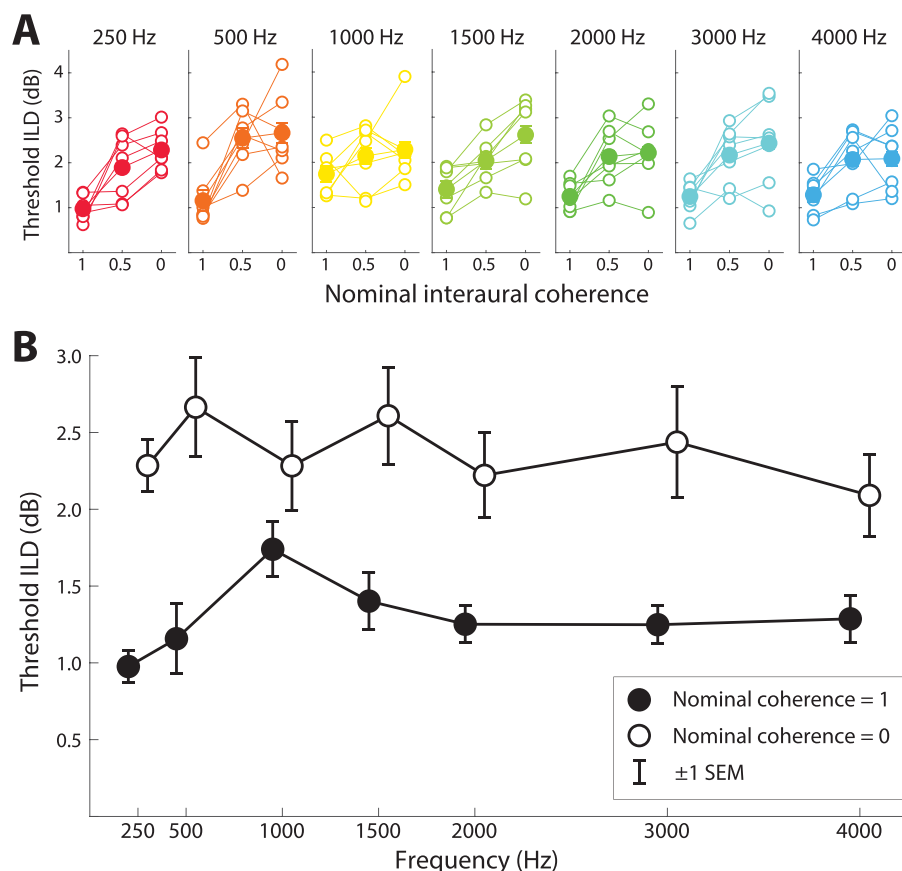


FIG. 2. (Color online) Experiment 1 discrimination data across frequency and nominal interaural correlation. (A) Individual discrimination thresholds (open symbols) and mean thresholds (filled symbols) for all tested frequencies (columns) across three levels of nominal interaural correlation. (B) Average discrimination thresholds across frequency for interaurally correlated (filled symbols) and uncorrelated (open symbols) stimuli. Errors bars indicate ± 1 standard error. Note that the nominal interaural coherence refers to the waveform correlation; the normalized envelope correlation for Experiment 1 stimuli was approximately 0.8 at a waveform correlation of 0.0 (see Sec. III B).

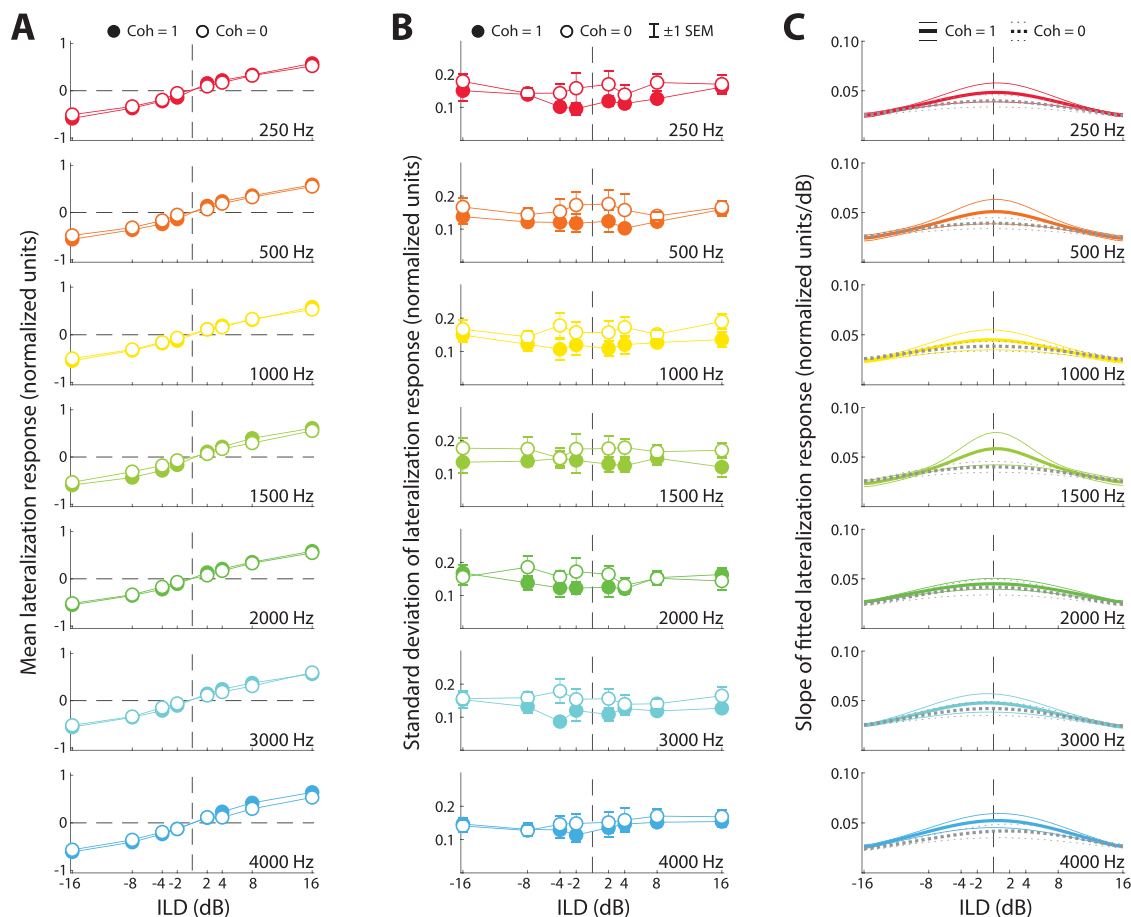


FIG. 3. (Color online) Experiment 1 average lateralization and lateralization variability. (A) Average lateralization response as a function of ILD for correlated (filled symbols) and uncorrelated (open symbols) stimuli. Data are plotted for ILDs near and beyond the discrimination threshold, i.e., ≥ 2 dB; each point gives the mean across seven subjects. (B) Lateralization response variability (standard deviation) as a function of ILD for correlated (filled symbols) and uncorrelated (open symbols) stimuli for trials with ILDs ≥ 2 dB. Errors bars indicate ± 1 standard error. (C) The local slope (gradient) of lateralization taken from sigmoidal fits to the lateralization responses summarized in (A). Solid lines plot the mean local slope for the correlated condition ± 1 standard error; dotted lines plot the mean local slope for the uncorrelated condition ± 1 standard error.

uncorrelated conditions. Figure 3(A) shows the mean lateralization responses for the correlated (filled symbols) and uncorrelated (open symbols) stimuli for ILDs ≥ 2 dB, i.e., magnitudes near and above the discrimination threshold. Responses were broadly similar for the two cases with lateralization changing systematically from left to right as a function of the ILD but some evidence of reduced lateralization for uncorrelated stimuli (open symbols show slightly smaller magnitudes in most cases), a point considered further below. Figure 3(B) shows average lateralization blur (see Sec. II) for correlated and uncorrelated stimuli across ILD (± 1 standard error). Blur generally appeared to be higher for uncorrelated than correlated stimuli. Consistent with this observation, a repeated-measures ANOVA with factors of frequency, correlation (correlated, uncorrelated), and ILD magnitude (2, 4, 8, and, 16 dB) indicated a significant main effect of correlation ($F_{1,6} = 9.59$, $p = 0.021$) on lateralization blur; other main effects and interactions were not significant ($p > 0.05$). That is, whereas suprathreshold ILDs effectively shifted the intracranial image away from the midline despite decorrelation, the image appeared to be relatively more diffuse, consistent with the subjective

reports of listeners (Hartmann and Constan, 2002; cf. Blauert and Lindemann, 1986; see Sec. V). The local slope of lateralization [Fig. 3(C)], taken as the gradient of sigmoidal fits to individual subject lateralization responses (two-parameter logistic), also appeared to be somewhat shallower near the midline for uncorrelated (dotted lines) than for correlated (solid lines) stimuli. This difference did not reach significance (repeated-measures ANOVA for local slope maxima, i.e., the peak in gradient about 0 dB ILD, with main factors of correlation and frequency, main effect of correlation $F_{1,6} = 4.28$, $p = 0.084$), suggesting that increased lateralization blur (see above) may have been the dominant contributor to reduced discrimination performance.

Concerning specifically the maximum extents of lateralization produced by correlated and decorrelated stimuli at the largest tested ILDs, Fig. 4(A) shows the lateralization range produced by stimuli across frequency and interaural correlation (individuals, open symbols; mean ± 1 standard error, filled symbols) expressed as the mean response magnitude at $|16$ dB ILD. Consistent with the pattern of performance shown in Fig. 3(A), the range of lateralization was

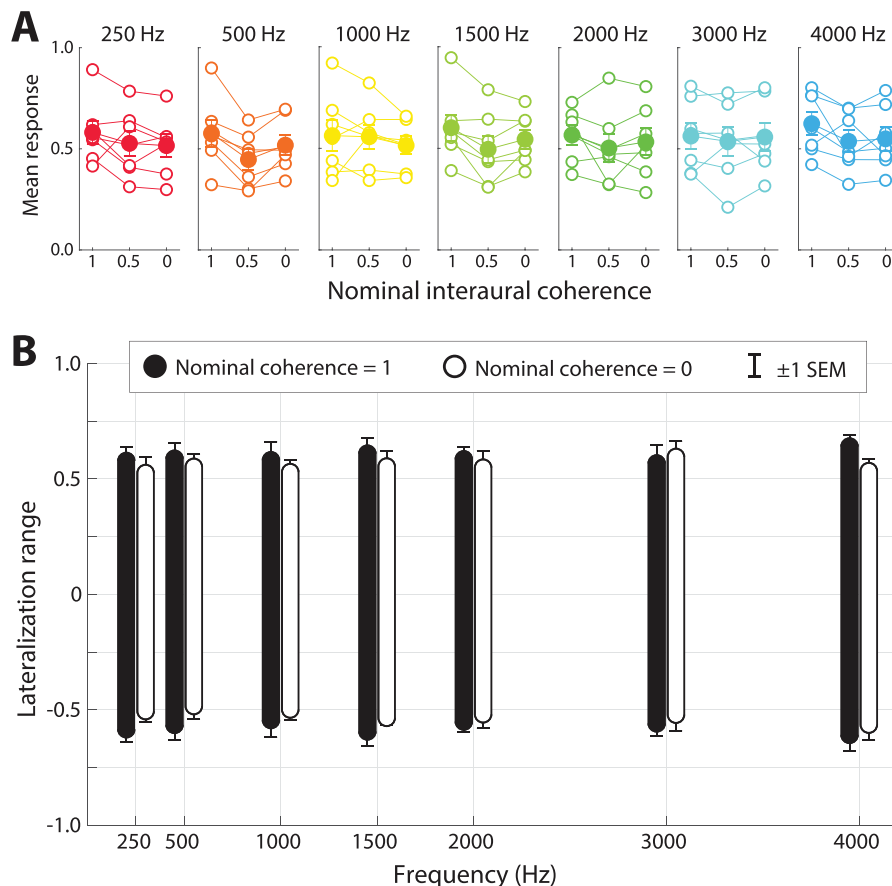


FIG. 4. (Color online) Experiment 1 range of lateralization across frequency and interaural correlation. (A) Format as in Fig. 2(A) but for lateralization range, defined as the difference in lateralization responses for the maximal rightward versus leftward ILDs. (B) Average lateralization ranges for correlated (filled bars) and uncorrelated (open bars) stimuli. The end point of each bar is at the average response elicited at -16 dB (lower end point) or $+16$ dB (upper end point) ILD with error bars indicating one standard error across seven subjects.

slightly compressed by decorrelation, with reduced lateralization range for both half-correlated and uncorrelated conditions at most frequencies. These data are summarized in Fig. 4(B) for correlated (black bars) and uncorrelated (white bars) conditions, with the vertical length of each bar giving the total lateralization range (± 1 standard error at each positive and negative end point). Lateralization range data, including the half-correlated data shown in Fig. 4(A), were submitted to a repeated-measures ANOVA with factors of frequency and interaural correlation. The main effect of interaural correlation was significant ($F_{2,8.1} = 10.68$, $p = 0.008$), whereas the main effect of frequency and the frequency-by-interaural correlation interaction were not ($p > 0.05$). The largest mean lateralization range occurred in the correlated condition at 4000 Hz, appearing somewhat larger than lateralization ranges at lower frequencies (cf. Bernstein and Trahiotis, 2011), but this difference did not reach significance.

B. Interim discussion

The foregoing data demonstrate that sensitivity to ILD is degraded when uncorrelated (temporally independent) signals are presented to the two ears within narrow frequency bands. ILD discrimination thresholds for uncorrelated stimuli were elevated by approximately 1–1.5 dB (re: correlated), and extents of laterality at suprathreshold ILDs were reduced by approximately 10%. The effect of

decorrelation appeared to be independent of frequency, although the mean decrement in performance at 1000 Hz (approximately 0.4 dB) was somewhat smaller than at other tested frequencies, owing to the relatively high threshold already present in the correlated condition (see Sec. V).

While the present data underscore the relative robustness of the ILD detection process, the observed magnitude of the effect of decorrelation on ILD discrimination for narrowband stimuli was roughly twice that reported by Hartmann and Constan (2002) for broadband or lowpass stimuli. The effect was similar to that observed in a previous study (Brown and Tollin, 2016) for narrowband high-frequency (4000 Hz) tokens with explicitly decorrelated 100-Hz narrowband noise envelopes. The frequency-independence of the decorrelated thresholds is notable, and we were initially puzzled that the effect observed here should be no larger at 250 Hz—where the average stimulus period is 4 ms such that uncorrelated signals are on average 1 ms out-of-phase—than at 4000 Hz—where uncorrelated signals are, on average, only $\sim 63 \mu\text{s}$ out-of-phase, and auditory coding of temporal fine structure is poor besides (e.g., Verschooten *et al.*, 2019).

Upon further examination, a fundamental constraint on the interpretation of measured performance was identified. Although stimulus *waveforms* were designed to be independent and such independence would be a prominent feature of resultant inputs to an ILD detection process, stimulus envelopes were also decorrelated: across a sample pool of 500 tokens per frequency, the mean normalized

envelope correlation was 0.81, approaching the theoretical minimum value of $\pi/4$ (see Aaronson and Hartmann, 2010). Because of the narrow stimulus bandwidth (25 Hz), intrinsic envelope fluctuations were both relatively prominent (stimulus crest factor approximately 2.7; envelope fourth moment approximately 1.9; see Sec. II) and slow enough to introduce, due to independently fluctuating levels at each ear, substantial and random fluctuation of ILD around the nominal ILD. When computed within a running 40-ms window, the standard deviation of time-varying ILD around the nominal ILD for a sample pool of 500 tokens per frequency was 5.0 dB.

Therefore, based on the results of Experiment 1 alone, it was not possible to determine which aspects of degraded ILD sensitivity were attributable to random envelope fluctuations introducing temporal variation of the nominal ILD cue versus decorrelation *per se*—that is, temporal independence of left- and right-ear signals disrupting the ILD detection process. To address this limitation, a second experiment leveraged low-fluctuation noise tokens (see Sec. II) to explicitly constrain envelope fluctuations and, correspondingly, limit ILD variation.

IV. EXPERIMENT 2: LOW-FLUCTUATION STIMULI

A. Psychophysical results

Figure 5 shows ILD discrimination thresholds for low-fluctuation stimuli in the format of Fig. 2 for a different

group of listeners [$n = 6$]; note that half-correlated stimuli were not presented in Experiment 2]. Thresholds in the correlated condition were similar to those observed in Experiment 1, including a mean threshold maximum at 1000 Hz, although the range of observed thresholds at 1000 Hz was relatively large, and the difference relative to adjacent frequencies was nonsignificant: one subject recorded a prominent maximum threshold ILD of 3.1 dB, while another subject recorded a *minimum* threshold of 0.6 dB. The inset panel of Fig. 5 shows the effect of removing either subject on the appearance of the 1000-Hz bump (cf. Mills, 1960; Yost and Dye, 1988; see Sec. V).

Regarding the main impetus for Experiment 2, the pattern of thresholds in the uncorrelated condition was markedly different from that in Experiment 1. Whereas thresholds were approximately doubled by decorrelation (to ~ 2.5 dB ILD) at frequencies of 250 and 500 Hz, the effect of decorrelation abruptly declined at higher frequencies and disappeared completely at frequencies ≥ 2 kHz. Correspondingly, a repeated-measures ANOVA with factors of correlation and frequency demonstrated significant main effects of both correlation ($F_{1,5} = 40.04$, $p = 0.001$) and frequency ($F_{2,4,11.9} = 7.28$, $p = 0.007$) and a significant frequency-by-correlation interaction ($F_{2,5,12.3} = 7.28$, $p = 0.004$). The effect of decorrelation was comparable at 250 Hz ($t_5 = 4.70$, $p = 0.005$) and 500 Hz ($t_5 = 3.91$, $p = 0.011$), dissipated at 1000 Hz ($t_5 = 1.98$, $p = 0.104$) and 1500 Hz ($t_5 = 2.40$, $p = 0.062$), and was entirely absent at

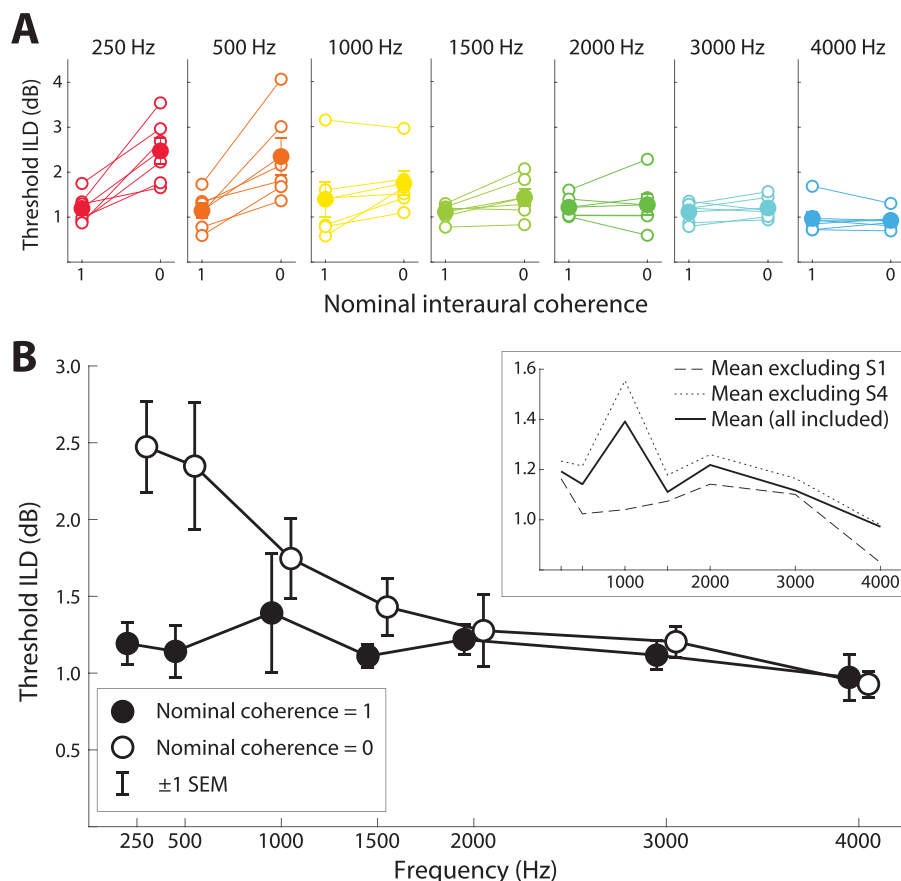


FIG. 5. (Color online) Experiment 2 discrimination data across frequency and nominal interaural correlation. (A) Legend as in Fig. 2(A). Note that via the low-fluctuation token generation procedure, the normalized envelope correlation was approximately 1.0 for all Experiment 2 stimuli (see Sec. IV B for more detailed analyses). (B) Legend as in Fig. 2(B) except inset: mean thresholds expanded for correlated stimuli only, illustrating the influence of two subjects on the appearance of the 1000-Hz bump (S1, threshold ILD at 1000 Hz = 3.1 dB; S4, threshold ILD at 1000 Hz = 0.6 dB; see text).

2000 Hz, 3000 Hz, and 4000 Hz (all mean threshold differences $<|0.1\text{ dB}|$, all $p \gg 0.05$).

Figure 6 shows lateralization for low-fluctuation stimuli in the format of Fig. 3. The effects of decorrelation were generally less apparent in Experiment 2 than in Experiment 1 for all lateralization metrics. Lateralization blur appeared to be increased by decorrelation in many cases, but to a lesser extent and less consistently than in Experiment 1. Lateralization magnitude [Fig. 6(A)] and slope [Fig. 6(C)] were slightly reduced for the decorrelated stimuli in Experiment 2 at 250 Hz, but effects were variable and/or of smaller magnitude at other frequencies. A repeated-measures ANOVA on lateralization blur with factors of correlation, ILD magnitude, and frequency indicated a significant main effect of correlation ($F_{1,5} = 10.40$, $p = 0.023$) but no other significant effects or interactions. A repeated-measures ANOVA on lateralization gradient indicated no main effect of correlation but a marginal frequency-by-correlation interaction ($F_{2,7,13.7} = 3.18$, $p = 0.061$) and also a significant main effect of frequency ($F_{2,0,10.2} = 7.05$, $p = 0.012$).

Concerning specifically the extents of laterality produced by low-fluctuation stimuli at the largest tested ILDs ($|16\text{ dB}|$), Fig. 7 plots the lateralization range data for Experiment 2 in the format of Fig. 4. A repeated-measures ANOVA on lateralization range indicated a nonsignificant

main effect of correlation ($F_{1,5} = 2.52$, $p = 0.174$) and only a marginal frequency-by-correlation interaction (after Greenhouse-Geisser correction, $F_{2,7,13.6} = 2.54$, $p = 0.104$) carried by the reduced range for uncorrelated stimuli at 250 Hz ($t_5 = 2.97$, $p = 0.031$). Notably, the ANOVA also demonstrated a significant main effect of frequency ($F_{2,4,11.8} = 6.85$, $p = 0.009$) with greater lateralization range at high frequencies than low frequencies (e.g., 4000 Hz versus 500 Hz for both the correlated ($t_5 = 4.19$, $p = 0.009$) and uncorrelated ($t_5 = 3.37$, $p = 0.020$) conditions; cf. Bernstein and Trahiotis, 2011).

B. Stimulus-based prediction of psychophysical results

Taken together, the data of Experiment 2 suggest a rather different conclusion than the data of Experiment 1: sensitivity to ILD is indeed impacted by decorrelation but, controlling for envelope fluctuations that impact the ILD itself, it is only appreciably impacted at the lowest of frequencies ($\approx 1000\text{ Hz}$ but especially $\leq 500\text{ Hz}$). Envelope fluctuations of Experiment 2 stimuli were very slight indeed: across a sample pool of 500 waveforms per frequency, the mean crest factor was 1.58 dB and the mean envelope fourth moment was 1.14. Correspondingly, demonstrating the similarity of left- and right-ear envelopes, the mean envelope

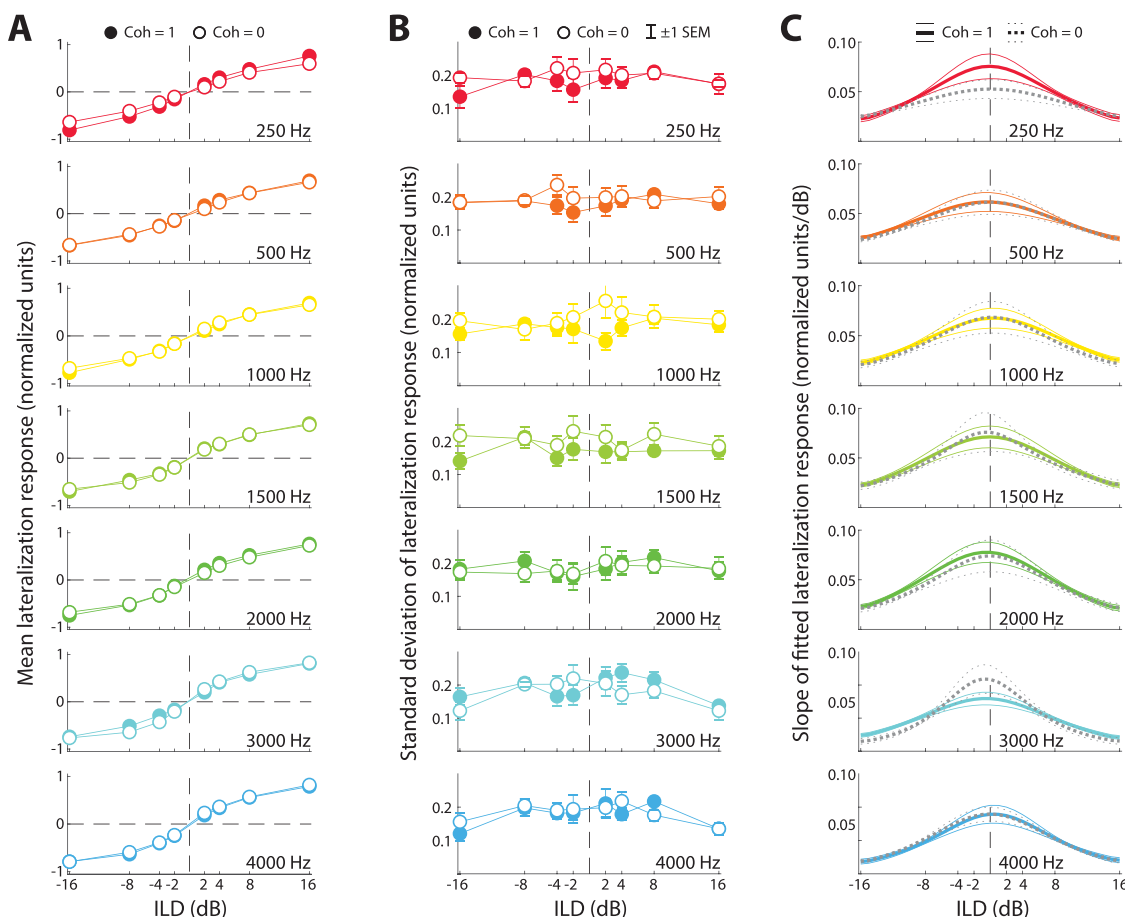


FIG. 6. (Color online) Experiment 2 average lateralization and lateralization variability. Legend otherwise as in Fig. 3.

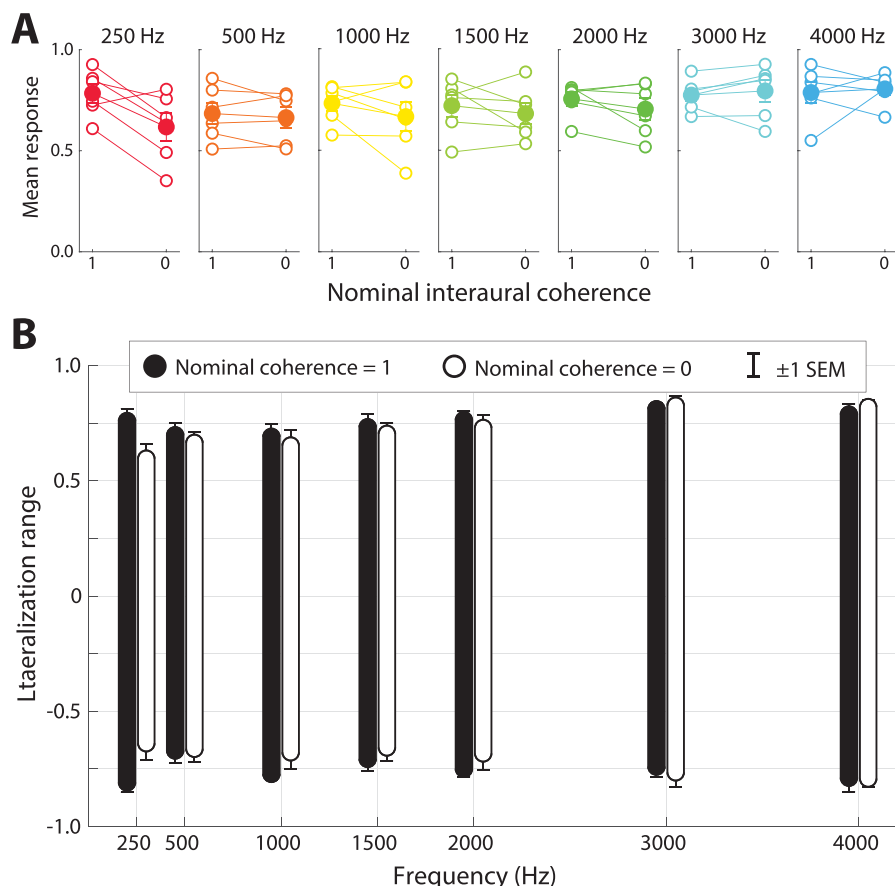


FIG. 7. (Color online) Experiment 2 range of lateralization across frequency and interaural correlation. Legend otherwise as in Fig. 4.

correlation of Experiment 2 stimuli was $0.997 (\pm 0.001$ standard deviation). In Secs. IV B 1–IV B 3, we consider to what extent the pattern of psychophysical responses across frequency can be accounted for by several features of the stimulus tokens presented. Here, we make few assumptions about auditory processes *per se*; contributions of such processes, including effective temporal windows of integration in ILD-computing neurons, are considered more explicitly in Sec. V.

1. Time-varying ILDs

All Experiment 2 stimulus tokens were stored for off-line quantification of binaural properties. We consider only uncorrelated tokens, for which binaural properties were subject to random variation, both across tokens and over time within a single token. Correlated tokens were identical across the ears; their binaural properties (ILD, ITD, and interaural correlation) were defined *a priori* and invariant within a given trial. In the uncorrelated condition, across trials, 320 unique tokens for each ear (640 total) were generated at each of 7 frequencies for a total of 4480 tokens per subject. Pooled across 6 subjects, the calculations presented here thus reflect 26880 low-fluctuation noise tokens comprising 13440 unique binaural signals.

Figure 8(A) plots exemplar binaural tokens at 250 Hz (upper panel) and 4000 Hz (lower panel), each with a long-term ILD of 0.125 dB (the smallest ILD magnitude tested). Right ear (red) and left ear (blue) waveforms are directly

overlaid to illustrate two points: (1) at the whole-waveform level, by design, an ILD is not apparent (given 0.125 dB magnitude), but (2) within sufficiently brief temporal windows and despite low-fluctuation envelopes, a “time-varying” ILD still fluctuates above and below the nominal whole-token value. The extent of such a fluctuation depends on the length of the temporal window considered and, also, for a given window length, the stimulus frequency. In effect, the ILD is more likely to be affected by random cycle-to-cycle variability within shorter windows and at lower frequencies, because either leads to fewer waveform cycles per window. To capture the effect of window length, ILDs were computed across a range of window lengths from 2.5 ms (which captures less than a full period at 250 Hz) to 40 ms (presumed to exceed the operative window of the ILD computation within the auditory system; see Sec. V).

Figure 8(B) shows distributions of computed ILD values across five different window lengths (as labeled) and for each window length, across the seven tested frequencies. Distributions were generated by subtracting the nominal trial ILD from the computed window ILDs and binning the resultant per-window values with a resolution of 0.1 dB. Distributions are plotted as the percentage of total windows falling into each bin. For example, for the 40 ms window at 4000 Hz, nearly 40% of windows fell into the ILD bin centered at 0.0 dB (bin edges at ± 0.05 dB ILD). Indeed, all distributions were centered at 0 dB, as approximately half of the window ILDs were randomly greater than the nominal

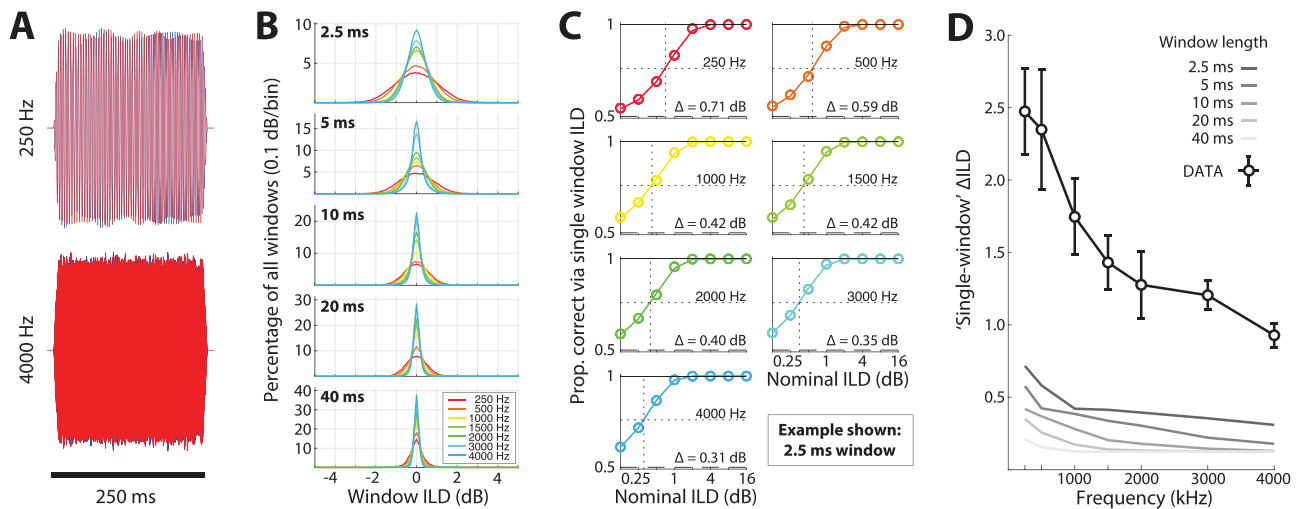


FIG. 8. Effect of time-varying ILDs conveyed by Experiment 2 stimuli. (A) Exemplar uncorrelated low-fluctuation noise tokens presented to the left ear (blue) and right ear (red) with a long-term ILD of 0.125 dB at 250 Hz (upper) and 4000 Hz (lower). (B) ILDs as computed within running temporal windows from 2.5 to 40 ms (as labeled) relative to the nominal (whole-token) ILD. Successive windows overlapped by 50% of the window duration. Values of per-window deviation were pooled across all trials/tokens of Experiment 2, binned with 0.1 dB resolution, and expressed as percentage of window deviations falling into each bin. (C) Discrimination performance of a “single-window” ILD detector, discriminating whole-waveform ILD on the basis of the ILD within a single 2.5 ms window (simulating an extreme form of non-uniform integration). Δ = threshold ILD. (D) Predicted Experiment 2 discrimination threshold ILDs (Δ ILD) obtained via a single-window ILD detector [as considered in (C)] for five different window lengths (grayscale lines). Empirical data (symbols) are plotted for comparison.

ILD and approximately half were less. As expected, shorter window length and lower frequency both resulted in greater ILD fluctuation (distribution width). While the magnitude of fluctuation was, in all cases, much lower than for Experiment 1 stimuli (see Sec. III B), notably, at smaller nominal ILD magnitudes and for sufficiently brief window lengths, some windows could carry a sign opposite that of the nominal ILD (e.g., given a nominal ILD of +0.5 dB, a deviation of −1 dB yields a window ILD of −0.5 dB). Thus, while the window ILD averaged across the duration of a given token faithfully tracked the nominal ILD—and an optimal ILD detector integrating evenly across each token would thus reach 100% discrimination performance—non-uniform integration could theoretically lead to incorrect discrimination of the nominal ILD due to spurious window ILDs.

Illustrating an extreme form of nonuniform integration, Fig. 8(C) plots the discrimination performance of an ILD detector operating on a single 2.5-ms window. For a given frequency, each sub-panel shows the proportion of trials (tokens) for which the detector correctly selected the sidedness (left or right) of the nominal ILD based on the window ILD. Discrimination thresholds (Δ), derived by the same method as psychophysical discrimination thresholds (Weibull fit at 76% correct), are given as insets within each panel. Consistent with the pattern of ILD variability shown in Fig. 8(B), performance is worst at the lowest tested frequency, 250 Hz, and steadily improves with increasing frequency. Performance also steadily improves with increasing window length because longer windows yield less ILD variability. Figure 8(D) shows the derived thresholds across all five simulated window lengths (grayscale; see inset legend)

as a function of the stimulus frequency using all presented stimuli in each case, effectively establishing a lower bound on performance based on stimulus variability alone. Observed psychophysical thresholds, including variability across subjects, are replotted on the same axes for comparison. Although this analysis suggests that nonuniform integration via a sufficiently brief window could constrain the discrimination of ILDs conveyed by Experiment 2 stimuli, even in the worst case (2.5 ms window, 250 Hz), single-window thresholds are severalfold better than psychophysical thresholds.

However, behavioral ILD discrimination is subject to uncertainty even for an invariant stimulus. Thus, the thresholds derived and plotted in Fig. 8 underestimate the thresholds expected given *both* stimulus variability and psychophysical uncertainty. Figure 9 plots predictions of ILD discrimination performance that consider both factors. Psychophysical uncertainty was derived, for each subject, from discrimination data for *correlated* Experiment 2 stimuli, i.e., stimuli for which ILDs were invariant. Specifically, each subject’s psychometric (Weibull) function (proportion correct versus ILD magnitude) per frequency was used to compute, for the specific window ILD values experienced by that subject, the probability that a response based on the window ILD would correctly discriminate the nominal (target) ILD. By this method, a new psychometric function could be fitted and ILD threshold derived, reflecting both stimulus (ILD) variability and psychophysical uncertainty. Such predictions, shown for a 2.5 ms window (the window length with the greatest variability), yield threshold ILDs for uncorrelated stimuli (gray diamonds) that are only slightly worse than thresholds for correlated stimuli (see below).

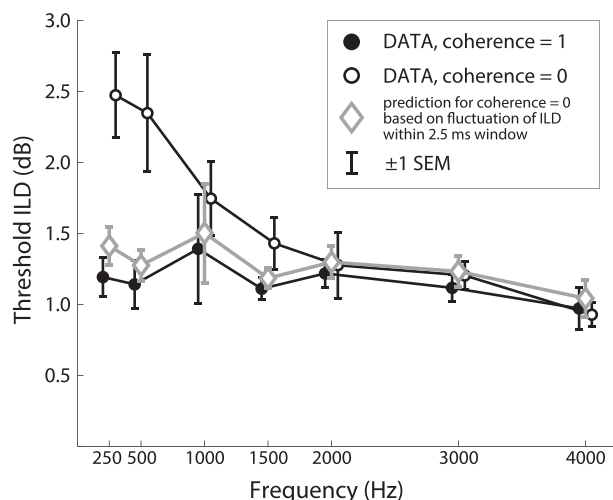


FIG. 9. Predicted “worst-case” discrimination of uncorrelated Experiment 2 stimuli for subjects impacted by ILD fluctuation only. Window ILDs conveyed by uncorrelated stimuli fluctuated around their nominal value, with fluctuation magnitude dependent on the window length considered [see Fig. 8(B)]. Gray diamonds plot predicted discrimination thresholds for an observer reliant on the ILD within a single fluctuating 2.5-ms window and susceptible to the same ILD uncertainty present for correlated stimuli (which do not convey fluctuating ILDs). Predicted thresholds are minimally elevated relative to observed correlated thresholds (filled circles) and substantially underestimate observed uncorrelated thresholds (open circles).

While the effect is slightly greater at low frequencies, the striking frequency-dependence observed in the empirical data is not evident.

In sum, stimulus ILD fluctuations do not appear sufficient to account for the observed psychophysical effect of interaural decorrelation at low frequencies, and any effects

of such fluctuation are estimated to be very slight indeed. While the low-fluctuation envelopes employed still produced randomly fluctuating ILDs (provided ILDs were calculated within sufficiently brief windows), the majority of window ILD fluctuations were still *sub-threshold*, i.e., fluctuating at magnitudes below the threshold ILD for correlated/invariant stimuli. Thus, even assuming highly non-uniform integration, the probability of a subject selecting the correct ILD was minimally affected by fluctuation: only occasionally would a large spurious ILD introduce a high probability of an incorrect response. The minimal predicted effect of ILD fluctuation is consistent with the lack of an effect of decorrelation at high frequencies (≥ 2 kHz) observed empirically. The failure to account for the observed effect of decorrelation at low frequencies pointed to the involvement of explicitly temporal factors as parsed in Secs. IV B 2 and IV B 3.

2. Time-varying ITDs

Uncorrelated stimuli of the present investigation carried no consistent long-term ITDs: by design, the peak of the whole-stimulus cross-correlation function (across all times) was near zero. However, sufficiently brief stimulus *segments* could convey large nonzero ITDs associated with prominent peaks in the cross correlation of left and right signal segments. Here, we consider to what extent such “covert” ITDs may have influenced psychophysical performance.

Figure 10(A) shows exemplar signal segments within a 2.5 ms window at 250 Hz (upper left) and 4000 Hz (lower left), each conveying a right-leading ITD. A plot of calculated ITDs (bin size 100 μ s) across window length and

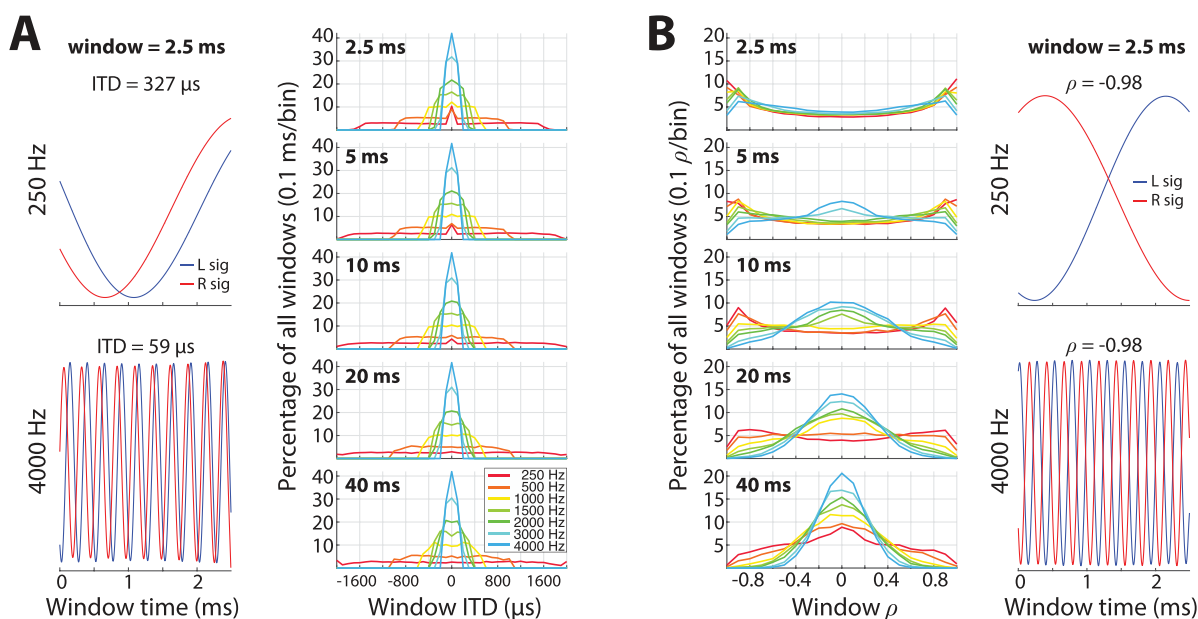


FIG. 10. Time-varying temporal features of Experiment 2 stimuli. (A) (Left) Exemplar 2.5-ms segments of uncorrelated low-fluctuation noise tokens presented to the left ear (blue) and right ear (red) at 250 Hz (upper) and 4000 Hz (lower). A nonzero ITD is conveyed in each case. (Right) ITDs as computed within running temporal windows from 2.5 to 40 ms (as labeled). Successive windows overlapped by 50% of the window duration. Values of ITD were pooled across all trials/tokens of Experiment 2, binned with 100 μ s resolution, and expressed as a percentage of window ITDs falling into each bin. (B) (Left) As in (A), right but for values of waveform correlation (ρ), naturally ranging from -1.0 (anticorrelated) to $+1.0$ (identical) and binned with 0.1 resolution. (Right) As in (A), left but illustrating windows in which the left and right signals are nearly anticorrelated.

stimulus frequency for all uncorrelated stimuli of Experiment 2 is also shown [Fig. 10(A), right; format otherwise as in Fig. 8(B)]. In all cases, window ITDs were taken as the lag (in μs) at the peak cross-correlation of left and right signal segments. Frequency-dependence of waveform ITD sensitivity aside (see Introduction and Sec. V), the range of ITDs randomly conveyed across windows is itself sharply frequency-dependent, naturally constrained by the stimulus period (note: in the present analysis, the maximum ITD is further constrained at 250 Hz for the 2.5 ms window size by the window length itself). Although window ITD distributions peaked at around 0 μs (bin edges at $\pm 50 \mu\text{s}$), window ITDs on the order of several hundred microseconds were quite common at low frequencies. Importantly, these momentary ITDs could be associated with high momentary interaural correlation values, as illustrated in Fig. 10(B) [values of the waveform interaural correlation (ρ) across temporal windows; format otherwise as in Fig. 10(A)]. That is, large and potentially *salient* ITDs could arise over brief periods within nominally “uncorrelated” low-frequency signals. [Additional details of Fig. 10(B), including the relevance of the correlation values ≤ 0 , will be treated in greater detail in Sec. IV B 3.]

The presence of ITD cues in a ILD detection task creates the possibility that subject responses may be influenced by ITD cues instead of or in addition to the target ILD, the cue on which the performance is evaluated. One means of assessing the extent of such influence is to use the computed window ITDs to predict the subject’s discrimination response on a per-trial basis. Via this method, windows for which the ITD is negative (left-leading) predict that the subject should respond “left” while positive ITDs predict that the subject should respond “right.” Windows with an ITD of zero make no prediction so can be randomly assigned left or right prediction values. By comparing the prediction of each window against the observed response, a d' value can be derived for each window. Finally, these d' values can be plotted as a function of the window time, indexing the influence of spurious ITDs across the stimulus duration. Window time is a principled organizing dimension, because stimulus ITD is known to be particularly potent near the stimulus onsets for a wide variety of signals (Saber, 1996; Freyman *et al.*, 1997; Brown and Stecker, 2010; Dietz *et al.*, 2013; Stecker and Bibee, 2014).

Figure 11(A) plots the predictive performance (d') of window ITD as a function of the window time across stimulus frequency (rows) and target ILD magnitude (columns). ITDs were computed within a sliding 2.5-ms window (50% overlap between adjacent windows). The resultant traces are termed temporal weighting functions (TWFs). TWFs were computed for individual subjects based on the unique set of ITD cues conveyed and responses obtained. Each plot shows the mean TWF (bold lines) ± 1 standard error (thin lines). Boxes highlight cases in which the upper bound (TWF mean + 1 standard error) for at least one window reached a $d' = 1$, i.e., 76% correct response prediction). Only the first 100 ms of each TWF is illustrated to enable better

visualization of temporal detail, and because the remaining 150 ms carried mean values in the vicinity of $d' = 0$ in all cases.

The influence of randomly occurring ITDs near the onsets of uncorrelated low-frequency stimuli is clear: for small ILD cue magnitudes (≤ 1 dB), subjects’ discrimination responses could be predicted via window ITDs near the stimulus onset (within the first ~ 10 ms) with mean TWFs approaching or exceeding $d' = 1$ within at least one window for all frequencies ≤ 1000 Hz. At the smallest tested ILD magnitude (0.125 dB), the earliest portion of the TWF also approached $d' = 1$ at 1500 Hz. Unsurprisingly, TWFs suggested no ITD influence at frequencies ≥ 2000 Hz, at which subjects are completely insensitive to waveform ITD (Zwislocki and Feldman, 1956; Brughera *et al.*, 2013). While envelope ITDs are detectable at higher frequencies (e.g., Henning, 1974), stimuli were gated on synchronously (10-ms \cos^2 ramp) and, by design, conveyed minimal envelope fluctuation (per metrics described previously). High-frequency TWFs calculated using envelope ITDs were found to be flat (ITDs had no predictive value), ostensibly owing to the weak envelope ITD cues conveyed (data not shown). TWFs were also generated using waveform ITDs computed using longer window lengths (5 ms, 10 ms, 20 ms, 40 ms): window lengths of 5–10 ms yielded TWFs similar in form but with less temporal detail, whereas window lengths of 20–40 ms began to flatten, ostensibly because computed “ITDs” reflected an increasingly decorrelated admixture of onset and post-onset signal segments (data not shown).

The influence of spurious onset ITD cues was most evident at the smallest ILD magnitudes (≤ 1 dB)—magnitudes near or below threshold ILDs measured for correlated stimuli. At larger ILD magnitudes, ITD generally appeared to exert little influence, and responses were instead predicted by the ILD. Figure 11(B) plots TWFs in the same format of Fig. 11(A), but computed using the window ILDs [again within a sliding 2.5-ms window; Fig. 8(B)]. TWFs are flat, suggesting that the ILD was similarly influential (predictive of discrimination responses) across the stimulus duration, though it is important to note that window ILDs and thus window predictions varied relatively little. That is, once the target ILD magnitude exceeded the range of the window ILD variation, virtually all windows would predict the same response, “correct” if the subject’s response matched the side of the target ILD and “incorrect” otherwise. At the larger ILD magnitudes, TWFs, increasingly flatter, took on steadily higher values, reaching $d' = \infty$ at a magnitude of 16 dB (illustrated here, for scaling purposes, at $d' = 4.65$, i.e., 99% correct). The boxes, again, highlight TWFs in which the upper bound of at least one window reached $d' = 1$. Relatively lower d' values for small ILD magnitudes at low frequencies are directly reflective of the decorrelation-elevated low-frequency ILD thresholds.

Considering both Figs. 11(A) and 11(B), two particular features of low-frequency TWFs bear further treatment. First, the ITD TWFs [Fig. 11(A)] at 1000 Hz are notable for

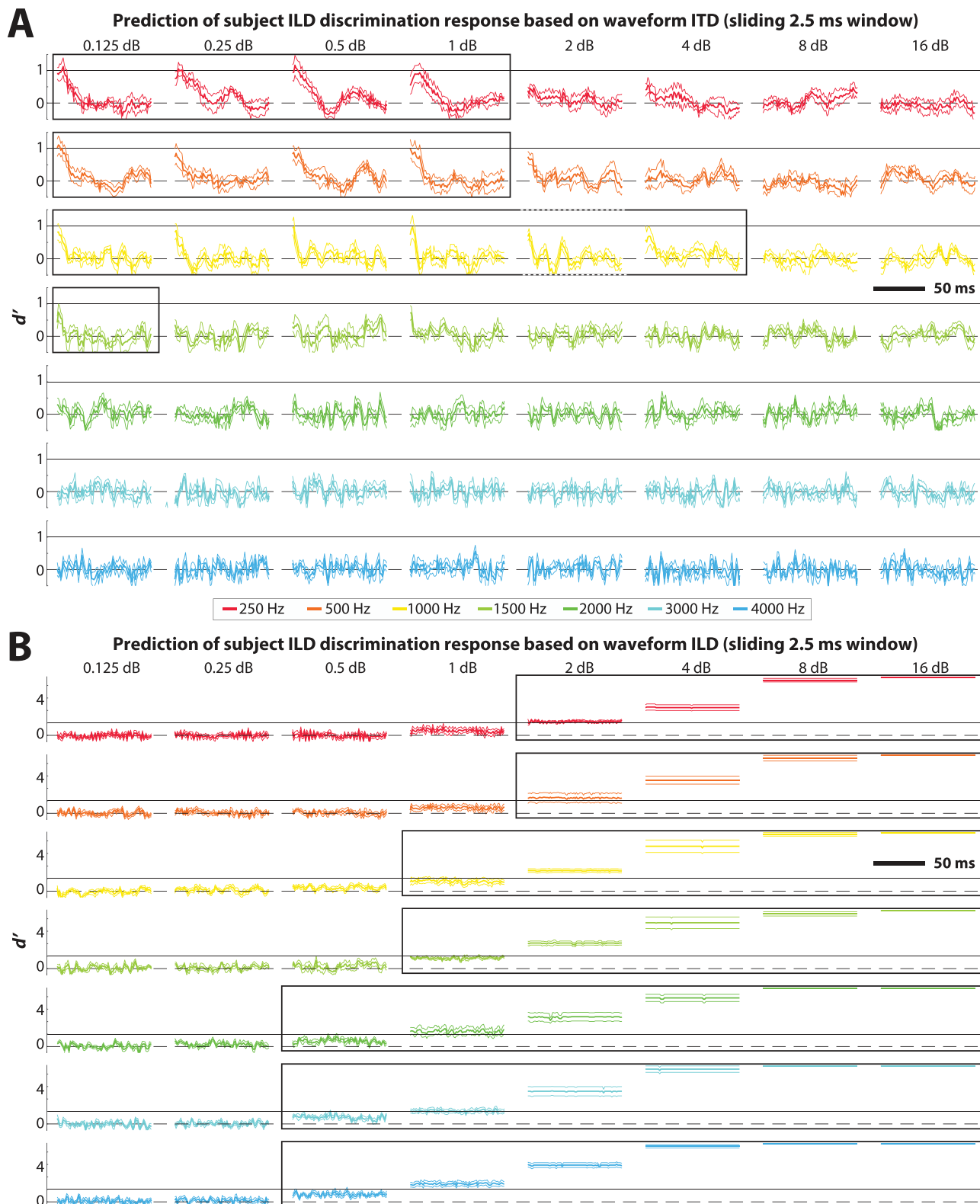


FIG. 11. Prediction of subject discrimination responses on the basis of randomly fluctuating cues within a running 2.5-ms window. (A) Across target ILD magnitude (columns) and frequency (rows), the accuracy with which per-window ITDs predicted per-trial subject ILD discrimination responses was quantified using d' to generate temporal weighting functions (TWFs; see text). Each TWF gives the mean d' value ± 1 standard error across the six subjects of Experiment 2 for successive 2.5-ms windows during the first 100 ms of the stimulus. Horizontal dashed lines demarcate $d' = 0$, indicating no predictive value (50% correct) while solid lines demarcate $d' = 1$, indicating 76% correct prediction. Boxes highlight TWFs in which the upper bound (mean TWF + 1 standard error) reached $d' = 1$ for at least one window. (B) For comparison, TWFs generated based on per-window ILDs are given in the format of (A) (note adjusted y-scale). The predictive value of ILD fluctuates comparatively little across the stimulus duration (ILD fluctuation was also comparatively slight), and values instead primarily reflect reliable responses in the direction of the target ILD at larger magnitudes (boxes), the cue upon which discrimination performance (Fig. 5) was evaluated.

the persistently elevated d' values near stimulus onset. The upper bound of the mean TWF (+1 standard error) approaches $d' = 1$ at an ILD magnitude of 2 dB and reaches $d' = 1$ at a ILD magnitude of 4 dB. A similar but lesser trend is evident at 500 Hz. That is, even as ILD exerted a greater influence with an increasing ILD magnitude [Fig. 11(B)] in this putative ILD discrimination task, onset ITDs continued to influence responses (see Sec. V). Second (and relatedly), at 500 Hz and especially 250 Hz, the influence of ITD appeared to dissipate with increasing ILD magnitude more abruptly than at 1000 Hz, even as ILD discrimination remained poorer—substantially—than at ≥ 1000 Hz. Indeed, the cross-frequency pattern of decorrelation-elevated threshold ILDs points to the involvement of a stimulus feature that most affected ILD processing at the lowest frequencies.

3. Time-varying correlation

As considered in Sec. IV B 2, the temporal relationship of left- and right-ear signals, as quantified within brief segments, varied over the stimulus duration. In fact, despite the uncorrelated nature of the stimulus tokens in the long-term, when computed within sufficiently brief windows, large nonzero values of correlation were inevitable. As shown in Fig. 10(B) across all of Experiment 2 tokens, large correlation magnitudes were more prevalent for shorter window lengths and at lower frequencies. Intuitively, for windows containing few waveform cycles (a function of both frequency and window length), correlation values near zero only occur when left and right signals are nearly orthogonal ($\pm 90^\circ$ relative phase). Otherwise, signals approaching homophasic or antiphase yield correlation magnitudes much greater than zero, occasionally near ± 1.0 . As window length or frequency increases, the contribution of random phase variation within the window increases, yielding a higher percentage of windows with low correlations.

The case of anticorrelation [resulting from randomly antiphase signal segments within a given window; illustrated in Fig. 10(B), right panel] is of particular interest. Whereas uncorrelated signals are orthogonal on average and thus out-of-phase by one-quarter of the stimulus period, moments of anticorrelation yield extreme interaural temporal mismatch equal to one-half of the stimulus period, naturally yielding the largest absolute mismatch at the lowest frequencies. For example, whereas anticorrelated signals at 4000 Hz are only mismatched by $\sim 125 \mu\text{s}$ —and even this mismatch is not preserved with fidelity due to limited high-frequency auditory phase-locking (e.g., Verschouten *et al.*, 2019)—anticorrelated signals at 250 Hz are mismatched by a full ~ 2 ms. Sufficient interaural temporal mismatch has been shown to disrupt the ILD computation in brainstem and midbrain neurons (Joris and Yin, 1995; Tollin, 2003; Brown and Tollin, 2016). The incidence of large (≥ 1 ms) temporal mismatches may, therefore, be expected to pose a particular challenge for ILD computation at low frequencies with the largest effects expected at the lowest frequencies.

This point and the collective implications of the foregoing data and analyses are considered in Sec. V.

V. GENERAL DISCUSSION

A. ILD detection is robust but not impervious to interaural decorrelation

This study considered two stimulus parameters previously shown to modestly influence ILD perception: interaural correlation and frequency. The most notable feature of the present data was the effect of interaural decorrelation on ILD discrimination, observed across frequency given stimuli with decorrelated envelopes (Experiment 1), but at low frequencies only given stimuli with “flat” envelopes (Experiment 2), for which stimulus timing information was conveyed exclusively (or nearly so) by the waveform. The effect of decorrelation across frequency for both experiments is summarized in Fig. 12 in both absolute (upper panel) and normalized sense (lower panel).

The data, in total, emphasize the robustness of the ILD detection process to even dramatic temporal degradation of its inputs (Hartmann and Constan, 2002; Devore and Delgutte, 2010; Brown and Tollin, 2016; cf. Egnor, 2001; Keating *et al.*, 2013). At its worst, the effect of decorrelation—of both the waveform and envelope (Experiment 1)—was to elevate ILD discrimination thresholds by approximately 1.5 dB. Although this represented more than a doubling of thresholds at the lowest frequencies tested, if projected into azimuthal (“spatial”) coordinates, the difference between detection at ~ 1 dB ILD and ~ 2.5 dB ILD is rather modest at most

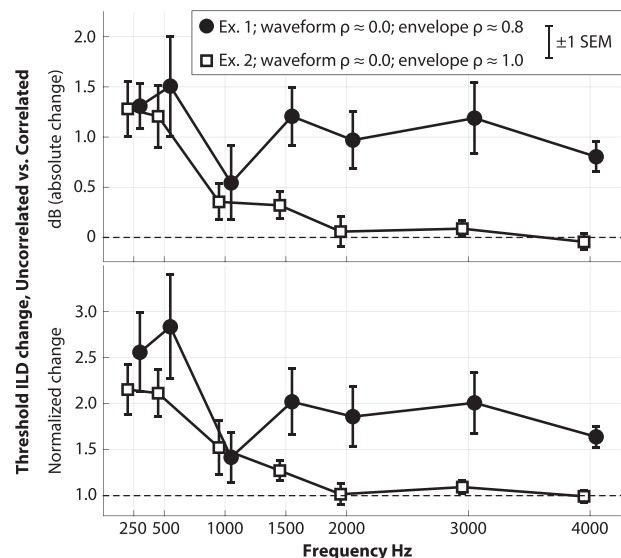


FIG. 12. Effect of decorrelation on ILD discrimination summarized. Per-subject discrimination thresholds for uncorrelated stimuli after subtraction of correlated thresholds, expressing the absolute effect of decorrelation within each experiment in terms of dB ILD (upper) or after division by correlated thresholds, expressing the normalized effect of decorrelation (lower). Mean effects for Experiment 1 (filled circles) and Experiment 2 (open squares) diverge at frequencies ≥ 1500 Hz, ostensibly owing to the marked reduction of the envelope fluctuations (and corresponding absence of envelope decorrelation) for “low-fluctuation” Experiment 2 stimuli (see text).

frequencies (e.g., Brungart and Rabinowitz, 1999). Thus, only modest spatial effects of decorrelation-reduced ILD sensitivity might be expected. In support of this expectation, lateralization of suprathreshold ILDs was also minimally affected by decorrelation with, at worst, an approximately 10% reduction in the extent of laterality reported. In cases of reduced lateralization, the variability of responses was also higher, consistent with a more diffuse intracranial percept (cf. Blauert and Lindemann, 1986; Hartmann and Constan, 2002).

Absent fluctuating envelopes—which certainly are a feature of many real-world signals, including the pulsatile signals experienced by ILD-reliant users of bilateral cochlear implants (e.g., Grantham *et al.*, 2008)—the effect of decorrelation on ILD detection appears to be relegated to low frequencies, primarily those ≤ 1000 Hz. We suggest that at least two separate factors contribute to this low-frequency bias. First, in uncorrelated stimuli of the present investigation, random ITDs unrelated to the target ILD arose within brief temporal windows due to the random phase relationships of the left and right waveforms. For low-frequency stimuli, particularly 500–1000 Hz, such ITDs arising near stimulus onset were predictive of subjects' discrimination responses despite the putative ILD target. This result is phenomenologically consistent with (1) the prime salience of low-frequency ITD cues as demonstrated in studies of binaural interference (cf. McFadden and Pasanen, 1976; Heller and Richards, 2010) and ITD/ILD trading (cf. Moushegian and Jeffress, 1959), (2) a large body of work demonstrating the potency of “onset” ITD (e.g., Saberi, 1996; Akeroyd and Bernstein, 2001; Dietz *et al.*, 2013; Stecker *et al.*, 2013; Stecker and Bibee, 2014), particularly when binaural information conveyed by the post-onset signal is sparse (e.g., Freyman *et al.*, 1997; Stecker, 2018), and (3) a separate body of work demonstrating that listeners are able to detect the ITD cues embedded in binaurally fluctuating and even uncorrelated signals (e.g., Grantham and Wightman, 1978; Bernstein *et al.*, 2001). However, whereas covert ITD cues appeared to be most salient at 1000 Hz and 500 Hz—the frequencies (among those tested here) for which ITD sensitivity is most acute (see Sec. VB)—ILD detection was most affected by decorrelation at the *lowest* frequency tested, 250 Hz—a frequency for which ITD sensitivity is not particularly acute [Zwislocki and Feldman, 1956; Brughera *et al.*, 2013; cf. Fig. 11(A)]. We suggest that a second factor fundamentally limits the detection of ILDs conveyed by stimuli in the low hundreds of Hz: millisecond-scale mistiming of phase-locked inputs to the ILD detection process.

Physiologically, ILD detection depends on integration of competitive excitatory and inhibitory inputs within a running temporal window (Joris and Yin, 1995; Park, 1998; Irvine *et al.*, 2001; reviewed in Tollin, 2003; Ashida *et al.*, 2017; Owruksy *et al.*, 2021). The length of this window depends on the auditory brain area under study, among other variables, but appears to be on the order of a few milliseconds by the level of the auditory midbrain (see Brown and Tollin, 2016). At frequencies in the thousands of Hz, even perfectly anticorrelated signals provide repeated excitatory

and inhibitory inputs within such a window, yielding an integrated output similar to that which would have been elicited with correlated (synchronous) inputs. Crossing into the hundreds and particularly low hundreds of Hz, the interaural temporal mismatch associated with decorrelation increases to a scale of milliseconds, and physiological models readily predict a decrement in ILD detection given mismatches of this magnitude (Brown and Tollin, 2016; see Ashida *et al.*, 2017). This effect is likely to dissipate in the vicinity of 1000 Hz as multiple peaks of even anticorrelated signals would fall within a common integration window. However, as described above, it is also in this spectral region that ITD *per se*, thought to depend on a separate neural detection process (see Grothe *et al.*, 2010), may exert its strongest perceptual influence.

B. A hypothesis on the origin of the 1000-Hz bump in threshold ILDs

As described in the Introduction, several studies over the past several decades have demonstrated, using tonal stimuli, a local maximum in threshold ILDs in the vicinity of 1000 Hz, i.e., the “1000 Hz bump.” This long-standing and as-yet unexplained nuance of binaural hearing was also evident in the present data (Figs. 2 and 5), although it was noted in the case of Experiment 2 that the peak was not significant and was particularly affected by one subject who recorded a prominent maximum threshold of 3.1 dB at 1000 Hz, while another subject recorded a *minimum* threshold of 0.6 dB. Indeed, taken across studies, it is evident that some listeners record a prominent maximum threshold at 1000 Hz, some record a maximum at a slightly different frequency (see below), and some record comparatively little fluctuation across frequency (Grantham, 1984; Goupell and Rosen, 2016; Goupell, 2021). Such variability suggests a need for further inquiry.

In Experiment 2, the trial-by-trial analysis of responses to interaurally decorrelated stimuli revealed that subjects' responses in a putative ILD discrimination task were affected by random covert ITD cues (visible only if computed using sufficiently brief temporal windows). The influence of ITD was most persistent across increasing ILD magnitude at 1000 Hz, slightly less so at 500 Hz, lesser still at 250 Hz, and least (nonzero) of all at 1500 Hz [Fig. 11(A)]. This cross-frequency pattern resembles that for ITD detection itself (Zwislocki and Feldman, 1956; Brughera, 2013) and is consistent with the perceptual potency of ITD cues in the 500–1000 Hz spectral region as demonstrated in a variety of tasks (see Sec. VA). It stands to reason that the same covert influence of ITD could affect measurements of “ILD discrimination” using stimuli that convey *diotic* ITD cues (including correlated stimuli of the present investigation). We thus offer the hypothesis that the maximum in ILD thresholds near 1000 Hz, first recorded by Mills (1960) and observed/replicated in a number of studies since, may simply coincide with the *minimum* in ITD thresholds near 1000 Hz, suggestive of an especially potent diotic cue in that spectral region.

Recent ITD data suggest that the minimum of the human ITD threshold-versus-frequency curve lies very near 1000 Hz indeed (Brughera *et al.*, 2013), but somewhat lower-frequency minima are sometimes suggested (cf. Stern and Shear, 1996). To this point, we did not present stimuli at frequencies intermediate to 500 and 1000 Hz, but the measurements of Grantham (1984) did demonstrate slightly lower-frequency ILD threshold maxima (800–900 Hz) in two of the four subjects of that study (in fact, only one of four subjects demonstrated a prominent “bump” at precisely 1000 Hz). Per our hypothesis, a diotic ITD cue should most effectively interfere with ILD detection at the frequency/frequencies for which ITD sensitivity is best, which naturally varies somewhat across listeners. Generally poorer ITD sensitivity would also predict a less potent diotic ITD influence, potentially decreasing the prominence of, or eliminating, the ILD bump. This hypothesis could be further tested with high-resolution measurements of both ITD and ILD thresholds across frequency in a common sample of listeners; covariation of the minimum ITD and maximum ILD thresholds within individual subjects would support our hypothesis, whereas a lack of covariation would challenge it.

Grantham (1984) suggested, as “one of probably several reasonable possibilities,” that the 1000 Hz bump might reflect a crossover of two different mechanisms for ILD coding, an intensity-to-time converter at low frequencies and a traditional intensity comparator at high frequencies. Although contributions of low-frequency intensity-time trading in ILD detection cannot be ruled out (e.g., Joris *et al.*, 2008), the suggestion that 1000 Hz (and lower frequencies) may be “too low for the system to utilize the intensity comparator with maximum efficiency” (Grantham, 1984) is not consistent with the finding that low-frequency ILD-sensitive neurons are functionally identical to high-frequency ILD-sensitive neurons (Jones *et al.*, 2015). Barring support for either this account of the 1000-Hz bump or our own, an explanation of this nuanced but intriguing detail of binaural hearing may require, as Grantham (1984) surmised, “a bit more imagination.”

C. Limitations of the present study

The present study pooled data across two relatively small groups of subjects ($n = 7$, $n = 6$) who were tested with different stimuli to provide insight on the combinatorial influences of the frequency and interaural correlation on sensitivity to ILD. Although measurements were completed at 21 different combinations of frequency-by-correlation, the stimulus space of interest is quite large and the resolution provided by the present data is thus limited. As the effect of the decorrelation *per se* disappears by 2000 Hz, consistent with a loss of access to the fine-structure binaural timing information, it would be desirable in the future to complete measurements with greater resolution at low frequencies. As the stimuli of the present investigation were fully synthetic and, particularly, in the case of

low-fluctuation stimuli, unnatural, it would also be desirable to obtain data with more ecological stimuli to provide more definitive insight on potential effects of decorrelation-reduced ILD sensitivity in real-world listening contexts.

ACKNOWLEDGMENTS

This work was supported by the National Institute for Deafness and Communication Disorders [National Institutes of Health (NIH) Grant Nos. R21-DC017213 (A.D.B.) and R01-DC011555 (D.J.T.)]. The authors wish to thank Dr. Leslie Bernstein and Dr. Chris Stecker for useful discussions and comments and Associate Editor Jonas Braasch and two anonymous reviewers for additional comments on an earlier version of this paper; Dr. Matthew Winn for insights concerning the generation of the experimental stimuli; Aoi Hunsaker, Christy Dong, Nicole Diebag, and Dr. Brianne Beemer for technical assistance; and P. Martin for facilitating a series of productive meetings that inspired this work.

- Aaronson, N. L., and Hartmann, W. M. (2010). “Interaural coherence for noise bands: Waveforms and envelopes,” *J. Acoust. Soc. Am.* **127**, 1367–1372.
- Akeroyd, M. A., and Bernstein, L. R. (2001). “The variation across time of sensitivity to interaural disparities: Behavioral measurements and quantitative analyses,” *J. Acoust. Soc. Am.* **110**, 2516–2526.
- Ashida, G., Tollin, D. J., and Kretzberg, J. (2017). “Physiological models of the lateral superior olive,” *PLoS Comput. Biol.* **13**, e1005903.
- Babkoff, H., Muchnik, C., Ben-David, N., Furst, M., Even-Zohar, S., and Hildesheimer, M. (2002). “Mapping lateralization of click trains in younger and older populations,” *Hear. Res.* **165**, 117–127.
- Bernstein, L. R., and Trahiotis, C. (2007). “Why do transposed stimuli enhance binaural processing?: Interaural envelope correlation vs envelope normalized fourth moment,” *J. Acoust. Soc. Am.* **121**, EL23–EL28.
- Bernstein, L. R., and Trahiotis, C. (2011). “Lateralization produced by interaural intensive disparities appears to be larger for high- vs low-frequency stimuli,” *J. Acoust. Soc. Am.* **129**, EL15–EL20.
- Bernstein, L. R., and Trahiotis, C. (2019). “No more than ‘slight’ hearing loss and degradations in binaural processing,” *J. Acoust. Soc. Am.* **145**, 2094–2102.
- Bernstein, L. R., Trahiotis, C., Akeroyd, M. A., and Hartung, K. (2001). “Sensitivity to brief changes of interaural time and interaural intensity,” *J. Acoust. Soc. Am.* **109**, 1604–1615.
- Blauert, J., and Lindemann, W. (1986). “Spatial mapping of intracranial auditory events for various degrees of interaural coherence,” *J. Acoust. Soc. Am.* **79**, 806–813.
- Brown, A. D., Benichoux, V., Jones, H. G., Anbuhl, K. L., and Tollin, D. J. (2018). “Spatial variation in signal and sensory precision both constrain auditory acuity at high frequencies,” *Hear. Res.* **370**, 65–73.
- Brown, A. D., and Stecker, G. C. (2010). “Temporal weighting of interaural time and level differences in high-rate click trains,” *J. Acoust. Soc. Am.* **128**, 332–341.
- Brown, A. D., Stecker, G. C., and Tollin, D. J. (2015). “The precedence effect in sound localization,” *J. Assoc. Res. Otolaryngol.* **16**, 1–28.
- Brown, A. D., and Tollin, D. J. (2016). “Slow temporal integration enables robust neural coding and perception of a cue to sound source location,” *J. Neurosci.* **36**, 9908–9921.
- Brughera, A., Dunai, L., and Hartmann, W. M. (2013). “Human interaural time difference thresholds for sine tones: The high-frequency limit,” *J. Acoust. Soc. Am.* **133**, 2839–2855.
- Brungart, D. S., and Rabinowitz, W. M. (1999). “Auditory localization of nearby sources: Head-related transfer functions,” *J. Acoust. Soc. Am.* **106**, 1465–1479.

- Carlile, S., Fox, A., Orchard-Mills, E., Leung, J., and Alais, D. (2016). "Six degrees of auditory spatial separation," *J. Assoc. Res. Otolaryngol.* **17**, 209–221.
- Devore, S., and Delgutte, B. (2010). "Effects of reverberation on the directional sensitivity of auditory neurons across the tonotopic axis: Influences of interaural time and level difference," *J. Neurosci.* **30**, 7826–7837.
- Devore, S., Ihlefeld, A., Hancock, K., Shinn-Cunningham, B., and Degutte, B. (2009). "Accurate sound localization in reverberant environments is mediated by robust encoding of spatial cues in the auditory midbrain," *Neuron* **62**, 123–134.
- Dietz, M., Marquardt, T., Salminen, N. H., and McAlpine, D. (2013). "Emphasis of spatial cues in the temporal fine structure during the rising segments of amplitude-modulated sounds," *Proc. Natl. Acad. Sci. U.S.A.* **110**, 15151–15156.
- Egnor, R. S. (2001). "Effects of binaural decorrelation on neural and behavioral processing of interaural level differences in the barn owl (*Tyto alba*)," *J. Comp. Physiol. A* **187**, 589–595.
- Freyman, R. L., Zurek, P. M., Balakrishnan, U., and Chiang, Y. C. (1997). "Onset dominance in lateralization," *J. Acoust. Soc. Am.* **101**, 1649–1659.
- Glasberg, B. R., and Moore, B. C. (1990). "Derivation of auditory filter shapes from notched-noise data," *Hear. Res.* **47**, 103–138.
- Goupell, M. (2021). (personal communication).
- Goupell, M. J., and Rosen, B. (2016). "Interaural level difference processing as a function of frequency," *J. Acoust. Soc. Am.* **140**, 3101.
- Grantham, D. W. (1984). "Interaural intensity discrimination: Insensitivity at 1000 Hz," *J. Acoust. Soc. Am.* **75**, 1191–1194.
- Grantham, D. W., Ashmead, D. H., Ricketts, T. A., Haynes, D. S., and Labadie, R. F. (2008). "Interaural time and level difference thresholds for acoustically presented signals in post-lingually deafened adults fitted with bilateral cochlear implants using CIS+ processing," *Ear Hear.* **29**, 33–44.
- Grantham, D. W., and Wightman, F. L. (1978). "Detectability of varying interaural temporal differences," *J. Acoust. Soc. Am.* **63**, 511–523.
- Grose, J. H., and Mamo, S. K. (2010). "Processing of temporal fine structure as a function of age," *Ear Hear.* **31**, 755–760.
- Grothe, B., Pecka, M., and McAlpine, D. (2010). "Mechanisms of sound localization in mammals," *Physiol. Rev.* **90**, 983–1012.
- Haftner, E. R., and Dye, R. H. (1983). "Detection of interaural differences of time in trains of high-frequency clicks as a function of interclick interval and number," *J. Acoust. Soc. Am.* **73**, 644–651.
- Haftner, E. R., Dye, R. H., Nuetzel, H. M., and Aronow, H. (1977). "Difference thresholds for interaural intensity," *J. Acoust. Soc. Am.* **61**, 829–834.
- Hartmann, W. M., and Cho, Y. J. (2011). "Generating partially correlated noise—A comparison of methods," *J. Acoust. Soc. Am.* **130**, 292–301.
- Hartmann, W. M., and Constan, Z. A. (2002). "Interaural level differences and the level-meter model," *J. Acoust. Soc. Am.* **112**, 1037–1043.
- Hartmann, W. M., and Pumphlin, J. (1988). "Noise power fluctuations and the masking of sine signals," *J. Acoust. Soc. Am.* **83**, 2277–2289.
- Hartmann, W. M., Rakerd, B., Crawford, Z. D., and Zhang, P. X. (2016). "Transaural experiments and a revised duplex theory for the localization of low-frequency tones," *J. Acoust. Soc. Am.* **139**, 968–985.
- Heller, L. M., and Richards, V. M. (2010). "Binaural interference in lateralization thresholds for interaural time and level differences," *J. Acoust. Soc. Am.* **128**, 310–319.
- Henning, G. B. (1974). "Detectability of interaural delay in high-frequency complex waveforms," *J. Acoust. Soc. Am.* **55**, 84–90.
- Irvine, D. R., Park, V. N., and McCormick, L. (2001). "Mechanisms underlying the sensitivity of neurons in the lateral superior olive to interaural intensity differences," *J. Neurophysiol.* **86**, 2647–2666.
- Jeffress, L. A., Blodgett, H. C., and Deatherage, B. H. (1962). "Effect of interaural correlation on the precision of centering a noise," *J. Acoust. Soc. Am.* **34**, 1122–1123.
- Jones, H. G., Brown, A. D., Koka, K., Thornton, J. L., and Tollin, D. J. (2015). "Sound frequency-invariant neural coding of a frequency-dependent cue to sound source location," *J. Neurophysiol.* **114**, 531–539.
- Joris, P. X., Michelet, P., Franken, T. P., and McLaughlin, M. (2008). "Variations on a dexterous theme: Peripheral time-intensity trading," *Hear. Res.* **238**, 49–57.
- Joris, P. X., and Yin, T. C. (1995). "Envelope coding in the lateral superior olive: I. Sensitivity to interaural time differences," *J. Neurophysiol.* **73**, 1043–1062.
- Keating, P., Nodal, F. R., Gananandan, K., Schulz, A. L., and King, A. J. (2013). "Behavioral sensitivity to broadband binaural localization cues in the ferret," *J. Assoc. Res. Otolaryngol.* **14**, 561–572.
- Kohlrausch, A., Fassel, R., van der Heijden, M., Kortekaas, R., van de Par, S., Oxenham, A. J., and Puschel, D. (1997). "Detection of tones in low-noise noise: Further evidence for the role of envelope fluctuations," *Acustica* **83**, 659–669.
- Licklider, J. C. R., and Dzendolet, E. (1948). "Oscillographic scatterplots illustrating various degrees of correlation," *Science* **107**, 121–124.
- Litovsky, R. Y., Jones, G. J., Agrawal, S., and van Hoesel, R. (2010). "Effect of age of onset of deafness on binaural sensitivity in electric hearing in humans," *J. Acoust. Soc. Am.* **127**, 400–414.
- Macpherson, E. A., and Middlebrooks, J. C. (2002). "Listener weighting of cues for lateral angle: The duplex theory of sound localization revisited," *J. Acoust. Soc. Am.* **101**, 2219–2236.
- McFadden, D., and Pasanen, E. G. (1976). "Lateralization at high frequencies based on interaural time differences," *J. Acoust. Soc. Am.* **59**, 634–639.
- Mills, A. W. (1960). "Lateralization of high-frequency tones," *J. Acoust. Soc. Am.* **32**, 132–134.
- Młynarski, W., and Jost, J. (2014). "Statistics of natural binaural sounds," *PLoS One* **9**, e108968.
- Moushegian, G., and Jeffress, L. A. (1959). "Role of interaural time and intensity differences in the lateralization of low-frequency tones," *J. Acoust. Soc. Am.* **31**, 1441–1445.
- Owruksy, Z. L., Benichoux, V., and Tollin, D. J. (2021). "Binaural hearing by the mammalian auditory brainstem: Joint coding of interaural level and time differences by the lateral superior olive," in *Binaural Hearing*, edited by R. Y. Litovsky, M. J. Goupell, R. R. Fay, and A. N. Popper (Springer International Publishing, Cham, Switzerland).
- Papesh, M. A., Folmer, R. L., and Gallun, F. J. (2017). "Cortical measures of binaural processing predict spatial release from masking performance," *Front. Hum. Neurosci.* **11**, 124.
- Park, T. J. (1998). "IID sensitivity differs between two principal centers in the internal intensity difference pathway: The LSO and the IC," *J. Neurophysiol.* **79**, 2416–2431.
- Pumphlin, J. (1985). "Low-noise noise," *J. Acoust. Soc. Am.* **78**, 100–104.
- Rakerd, B., and Hartmann, W. M. (1985). "Localization of sound in rooms. II. The effects of a single reflecting surface," *J. Acoust. Soc. Am.* **78**, 524–533.
- Rakerd, B., and Hartmann, W. M. (2010). "Localization of sound in rooms. V. Binaural coherence and human sensitivity to interaural time differences in noise," *J. Acoust. Soc. Am.* **128**, 3052–3063.
- Rayleigh, L. (1907). "On our perception of sound direction," *Philos. Mag.* **13**, 214–232.
- Rice, S. O. (1954). "Mathematical analysis of random noise," in *Selected Papers on Noise and Stochastic Processes*, edited by N. Wax (Dover, New York).
- Saberi, K. (1996). "Observer weighting of interaural delays in filtered impulses," *Percept. Psychophys.* **58**, 1037–1046.
- Stecker, G. C. (2018). "Temporal weighting functions for interaural time and level differences. V. Modulated noise carriers," *J. Acoust. Soc. Am.* **143**, 686–695.
- Stecker, G. C., Bernstein, L. R., and Brown, A. D. (2021). "Binaural hearing with temporally complex signals," in *Binaural Hearing*, edited by R. Y. Litovsky, M. J. Goupell, R. R. Fay, and A. N. Popper (Springer International Publishing, Cham, Switzerland).
- Stecker, G. C., and Bibee, J. M. (2014). "Nonuniform temporal weighting of interaural time differences in 500 Hz tones," *J. Acoust. Soc. Am.* **135**, 3541–3547.
- Stecker, G. C., and Brown, A. D. (2012). "Onset- and offset-specific effects in interaural level difference discrimination," *J. Acoust. Soc. Am.* **132**, 1573–1580.
- Stecker, G. C., Ostreicher, J. D., and Brown, A. D. (2013). "Temporal weighting functions for interaural time and level differences. III. Temporal weighting for lateral position judgments," *J. Acoust. Soc. Am.* **134**, 1242–1252.

- Stern, R. M., and Shear, G. D. (1996). "Lateralization and detection of low-frequency binaural stimuli: Effects of distribution of internal delay," *J. Acoust. Soc. Am.* **100**, 2278–2288.
- Tollin, D. J. (2003). "The lateral superior olive: A function role in sound source localization," *Neuroscientist* **9**, 127–143.
- Verschooten, E., Shamma, S., Oxenham, A. J., Moore, B. C. J., Joris, P. X., Heinz, M. G., and Plack, C. J. (2019). "The upper frequency limit for the use of phase locking to code temporal fine structure in humans: A compilation of viewpoints," *Hear. Res.* **377**, 109–121.
- Wichmann, F. A., and Hill, N. J. (2001). "The psychometric function: I. Fitting, sampling, and goodness of fit," *Percept. Psychophys.* **63**, 1293–1313.
- Wightman, F. L., and Kistler, D. J. (1992). "The dominant role of low-frequency interaural time differences in sound localization," *J. Acoust. Soc. Am.* **91**, 1648–1661.
- Yost, W. A., and Dye, R. H., Jr. (1988). "Discrimination of interaural differences of level as a function of frequency," *J. Acoust. Soc. Am.* **83**, 1846–1851.
- Zwislocki, J., and Feldman, R. S. (1956). "Just noticeable differences in dichotic phase," *J. Acoust. Soc. Am.* **28**, 860–864.